UNIVERSITY OF OKLAHOMA

GRADUATE COLLEGE

ESTIMATION AND ANALYSIS OF ATMOSPHERIC VORTICES

A DISSERTATION

SUBMITTED TO THE GRADUATE FACULTY

in partial fulfillment of the requirements for the

Degree of

DOCTOR OF PHILOSOPHY

By

LYNN GREENLEAF
Norman, Oklahoma
2013

ESTIMATION AND ANALYSIS OF
ATMOSPHERIC VORTICES

A DISSERTATION APPROVED FOR THE
DEPARTMENT OF MATHEMATICS

BY

Dr. Luther White, Chair

Dr. Alan Shapiro

Dr. Nikola Petrov

Dr. Kevin Grasse

Dr. Christian Remling

Acknowledgements

I would like to express my deepest appreciation to my committee chair, Dr. Luther White, without whose guidance and help this dissertation would not have been possible. His encouragement, insight and sincerity greatly affected me as a graduate student.

I would also like to thank Mr. Vincent T. Wood who provided me with the Davies-Jones data set used in this dissertation. He always found time to provide meteorological guidance. His scholarship proved valuable on many occasions.

Finally, I wish to express my gratitude to my husband, Garry Greenleaf, and my children, James and Tamara Greenleaf, for their love and support. Their encouragement and advice are greatly appreciated.

Contents

1 Introduction **1**

2 Fluid Mechanics **5**

2.1 Eulerean and Langrangian Descriptions 5

2.2 Navier-Stokes Equations 6

2.3 Vorticity and Circulation 11

3 Tangential Wind Models **13**

4 The Data Set **20**

5 The Forward Problem **22**

5.1 Cylindrical Case 23

5.2 NonCylindrical Case 25

6 The Inverse Problem **29**

6.1 Z-Dependent Profile Parameters 30

6.2 Tangential Profile Parameters 31

6.3 Determination of the Parameter ν 33

6.4 Analysis of the Residuals 33

6.4.1 Runs Test 34

6.4.2 Correlated Residuals 35

6.4.3 Normality Tests 36

6.5 Probability Distributions 42

6.6 Random Samples 43

6.6.1 Sample from a Grid 43
6.6.2 Gibbs Sample 44
6.6.3 Quasi-Monte Carlo Sample 44

7 Uncertainty Analysis **46**
7.1 Information Theory 46
7.2 Sensitivity Analysis 49
7.2.1 Local Sensitivity Analysis 50
7.2.2 Variance-Based Sensitivity Analysis 53

8 Estimation and Analysis of the Wood-White Vortex 2 Tangential Wind Model **57**
8.1 Parameters of ϕ 58
8.2 Tangential Wind v Through the Model ϕ 64
8.3 Radial Wind u 74
8.4 Vertical Wind w 83

9 Conclusions **90**

Appendices **97**

A Derivatives of the Vertical Wind Profile **98**

List of Figures

6.1 z-Profile fitted to Davies-Jones 31

8.1 Example joint pdfs for a and b 59

8.2 Marginal pdfs for a and b 59

8.3 Tangential Profile and Residual Plots 64

8.4 Autocorrelation Function at Level $z = 1$ 66

8.5 Residual and Normal cdfs, KS Test Statistic 67

8.6 Tangential cdf and Error Bars 70

8.7 Pseudo-random sample and Gibbs c.d.f.s 71

8.8 Local Sensitivity Coefficients 72

8.9 v with Approximate Error Bars 73

8.10 Radial Wind Profile: Cylindrical Case 74

8.11 Radial Wind Profile and Residuals 76

8.12 Residual and Normal cdfs, KS Test Statistic 78

8.13 Radial cdf and Error Bars 81

8.14 Pseudo-random sample and Gibbs c.d.f.s 82

8.15 Local Sensitivity with repect to ν 83

8.16 Vertical Wind Profile: Cylindrical Case 83

8.17 Vertical Wind Profile and Residuals 84

8.18 Residual and Normal cdfs, KS Test Statistic 85

8.19 Vertical cdf and Error Bars 87

8.20 Pseudo-random sample and Gibbs c.d.f.s 88

List of Tables

8.1 Optimal Parameters 58

8.2 Statistics for the Parameters 59

8.3 Information Content of Parameters 60

8.4 Variance-based Sensitivity for the Parameters 61

8.5 Uniform Distribution for the Parameters 62

8.6 Distribution Defined by DJ Data, Level 1 62

8.7 Distribution Defined by DJ Data, Level 2 62

8.8 Distribution Defined by DJ Data, Level 3 63

8.9 Statistics for Random Samples, level $z = 1$ 63

8.10 Statistics of the Residuals 65

8.11 Runs Test Statistics 65

8.12 Normality Test Statistics 66

8.13 Statistics for v, Grid Sample 68

8.14 Statistics for v, Pseudo-Random Sample 69

8.15 Statistics for v from Small Samples 71

8.16 Statistics of the Residuals 77

8.17 Normality Test Statistics 77

8.18 Statistics for u, Grid Sample 79

8.19 Statistics for u, Pseudo-Random Sample 80

8.20 Statistics for u from Small Samples 82

8.21 Statistics of the Residuals 84

8.22 Normality Test Statistics 85

8.23 Statistics for w, Grid Sample 86
8.24 Statistics for w, Pseudo-Random Sample 86
8.25 Statistics for w from Small Samples 87

9.1 Information with Two Different Samples 93

Abstract

Intense atmospheric vortices occur in dust devils, waterspouts, tornadoes, mesocyclones and tropical cyclones. Tangential wind models have been proposed that approximate the observed tangential wind profile of an atmospheric vortex for the purpose of data analysis and prediction. Data analysis is required to demonstrate in an objective way that a parameterized tangential wind model provides an acceptable description of the tangential wind profile of an atmospheric vortex and determine if the model can be used to make accurate predictions. Analysis of the residuals indicates that nonlinear least squares analysis is appropriate. The Wood-White 2 vortex model provides good approximations to the benchmark Davies-Jones data set in radial, tangential and vertical wind estimates. Using the methodology of Information Theory and Sensitivity Analysis, information content of the parameters of the Wood-White 2 vortex model show that both parameters are essential in estimation of the tangential wind profile. The variances in both parameters were large, but can be reduced by using random samples containing the statistical properties of the data. The Local Sensitivity Analysis method can be used without much loss of information which will be valuable in the analysis of models with a large number of parameters. Uncertainty in radial, tangential and vertical winds were examined and can be used effectively to predict these quantities and their uncertainties.

Chapter 1

Introduction

Intense atmospheric vortices occur in dust devils, waterspouts, tornadoes, mesocyclones and tropical cyclones. Tangential wind models have been proposed that approximate the observed tangential wind profile of an atmospheric vortex for the purpose of data analysis and prediction. Observations of tangential wind come from many sources, such as numerical simulations and mobile Doppler radar. Data analysis is required to demonstrate in an objective way that a parameterized tangential wind model provides an acceptable description of the tangential wind profile of an atmospheric vortex and determine if the model can be used to make accurate predictions. The problem of prediction is called the forward problem.

The tangential wind profiles of atmospheric vortices are often approximated by continuous nonlinear functions that are zero at the vortex center, increase to a maximum at some radius and then decrease asymptotically to zero. Atmospheric models are, in general, highly nonlinear. This is especially true for models of atmospheric vortices. The atmosphere is modeled as a fluid using the Navier-Stokes system of partial differential equations with practical solutions that are often nonlinear. A number of models, such as the idealized, inviscid Rankine (1882) [19], the viscous Burgers (1948) [4] -Rott(1958) [20] and Sullivan (1959) [26] analytical vortex models have been used to approximate observed profiles of tangential winds. New models have been proposed by Wood-White

(2011) [32] that use a rational function to model an inner core of solid-body rotation and an outer profile that decays to zero at infinity. The various models for tangential winds have parameters that contain useful information about the physical structure of a vortex. The parameters of any model must be assumed or estimated and often represent physical properties of the physical system. In the case of atmospheric vortices, parameters represent physical properties such as viscosity, interior rotational core flow, exterior potential rotational flow, circulation strength and strength of suction. The problem of using the results of some measurements to infer the values of parameters of the model is called the inverse problem. The state of information over the parameter space is central to the solution of the forward problem of prediction and the inverse problem of parameter resolution.

The forward and inverse problems are solved using probability and information theory, hence parameter estimation includes a priori information and information contained in data. Since there are a small finite number of parameters in the tangential wind models, the actual a posteriori probability density function is calculated as a solution to the inverse problem. This a posteriori probability density function incorporates any prior information assumed about the parameters in the tangential wind models as well as the information contained in the data. The forward problem then consists of evaluation of the flow of information into prediction of other quantities such as such as radial and vertical winds and the vortex pressure field. This approach makes is possible to determine vortex structure when there is incomplete data.

In this paper, analytic vortex models are used to estimate the tangential wind component of the vortex. This estimate is dependent on parameters which are

obtained by optimization techniques. With the a posteriori probability density function, statistical and information theory are used to analyze the resolution of the parameters, followed by a sensitivity analysis. Equations from the Navier-Stokes system of equations are used to estimate the radial and vertical wind components of the vortex, as well as the pressure differential along with an analysis of the flow of information into these quantities.

The thesis is organized in chapters as follows:

Chapter 2 addresses the essential elements of Fluid Mechanics that provide the fundamental background to this work.

Chapter 3 contains a list of tangential wind models that are of interest to meteorologists. The normalized Wood-White vortex 2 was selected for analysis because of its small number of parameters and its ability to capture the information in the data set providing the ability to do a thorough analysis.

Chapter 4 describes the Davies-Jones [11] benchmark data set. A benchmark data set is defined to be information that is believed to be accurate or true for use in comparing this information with computational results, and logical procedures for drawing conclusions from these comparisons [30].

Chapter 5 consists of the equations and methodology used to address the prediction problem.

Chapter 6 consists of the equations and methodology used to address the inverse problem of parameter prediction and resolution. This chapter discusses the parameters of the radial, tangential and vertical wind models and the z-dependent profile which models the vertical maximum tangential wind.

Chapter 7 addresses two topics that are essential in the forward and inverse problems. The first topic is Information Theory which defines the state of information over the parameter space and the propagation of information into quantities dependent on the parameters. The second topic is Sensitivity Anal-

ysis. Local Sensitivity Analysis concentrates on the local impact of the factors on the model and is usually carried out by computing partial derivatives of the output functions with respect to the input variables. Variance-Based Sensitivity Analysis is a global method that apportions the output uncertainty to the uncertainty in the input factors [22]. This is usually done by probability density functions defined on the admissible set of parameters, thus the technique incorporates the influence of the whole range of variation and the form of the probability density function of the input.

Chapter 8 gives the main results and contributions. Analysis of the residuals indicates that nonlinear least squares analysis is appropriate. The Wood-White 2 vortex model provides good approximations to the benchmark Davies-Jones data set in radial, tangential and vertical wind estimates. Using the methodology of Information Theory and Sensitivity Analysis, information content of the parameters of the Wood-White 2 vortex model show that both parameters are essential in estimation of the tangential wind profile. The variances in both parameters were large, but can be reduced by using random samples containing the statistical properties of the data. The Local Sensitivity Analysis method can be used without much loss of information which will be valuable in the analysis of models with a large number of parameters. Uncertainty in radial, tangential and vertical winds were examined and can be used effectively in a real-time system to predict these quantities and their uncertainties.

Chapter 9 contains the conclusions and recommends some potential topics for further research.

Chapter 2

Fluid Mechanics

2.1 Eulerean and Langrangian Descriptions

Atmospheric flow is a special case of fluid flow and can be described in two different ways. In the Lagrangian system, the observer follows an individual parcel or "bubble". This is the usual point of view of physics and calculus. In contrast, atmospheric dynamics is usually concerned with a specific location in space. In this Eulerian system, the observer is focused on a particular location. Since physical laws are usually given in terms of the Lagrangian description, it is important to derive the corresponding Eulerian destription.

The Lagrangian description in Cartesian coordinates will be given first. Let $\mathbf{r}(t) = (x(t), y(t), z(t))$ denote the position at time t of the "bubble", velocity $\mathbf{v}(t) = (u(t), v(t), w(t)) = (\frac{dx}{dt}, \frac{dy}{dt}, \frac{dz}{dt})$ denote the velocity at time t of the "bubble" and $\frac{D\mathbf{v}(t)}{Dt}$ denote the acceleration. The Eulerian description is given in terms of position $\mathbf{r}(t)$ and time t as $\mathbf{v}(\mathbf{r}(t), t)$ with acceleration $\frac{\partial \mathbf{v}(t)}{\partial t}$. By the Chain Rule:

$$\frac{D\mathbf{v}(t)}{Dt} \qquad \text{Lagrangian derivative}$$
$$= \frac{\partial \mathbf{v}(t)}{\partial t} \qquad \text{local acceleration of "bubble"}$$
$$+ (\mathbf{v} \cdot \nabla)\mathbf{v} \qquad \text{flow of the fluid}$$

where ∇ is the gradient operator

$$\nabla = (\frac{\partial}{\partial x}, \frac{\partial}{\partial y}, \frac{\partial}{\partial z})$$

2.2 Navier-Stokes Equations

Newton's second law (conservation of momentum) states that

$$\mathbf{F} = m\mathbf{a} = m\frac{D\mathbf{v}}{Dt} = \frac{Dm\mathbf{v}}{Dt}$$

Therefore, Newton's law states that the rate of change of momentum is determined by the forces acting on the body. The Navier-Stokes equations arise from applying Newton's second law in conjunction with conservation of mass and are used in physics to describe atmospheric motion. There are two types of forces on an air parcel: body forces such as the gravitational force and surface or stress forces. Surface forces are those that are exerted on an area element by direct contact. In this case, Newton's second law gives Cauchy's equation of motion:

$$\rho\frac{D\mathbf{v}}{Dt} = \rho\mathbf{g} + \frac{\partial \tau}{\partial \mathbf{x}}$$

where ρ is the density of air, $\mathbf{g}$ is the gravitational force vector and τ is the second order stress tensor. The relation between stress and deformation in a continuum is called a constitutive equation. It is assumed that in the

atmosphere, surface stress does not depend on the orientation of the surface. In other words, the stress tensor is isotropic or spherically symmetric. Therefore, the assumed constitutive relation for the stress tensor is of the form

$$\tau = -p\delta + \sigma$$

where p is the thermodynamic pressure. σ is the deviatoric stress tensor which is the stress due to motion and δ is the Kronecker delta tensor defined by

$$\delta = \begin{bmatrix} 1 & 0 & 0 \\ 0 & 1 & 0 \\ 0 & 0 & 1 \end{bmatrix}$$

Under the Newtonian hypothesis, the relationship between deviatoric stress and rate of strain is assumed linear and therefore if K is a fourth order tensor and e is the second order rate of strain tensor defined by

$$\mathbf{e} = \begin{bmatrix} \frac{\partial u}{\partial x} & \frac{1}{2}\left(\frac{\partial u}{\partial y} + \frac{\partial v}{\partial x}\right) & \frac{1}{2}\left(\frac{\partial u}{\partial z} + \frac{\partial w}{\partial x}\right) \\ \frac{1}{2}\left(\frac{\partial u}{\partial y} + \frac{\partial v}{\partial x}\right) & \frac{\partial v}{\partial y} & \frac{1}{2}\left(\frac{\partial v}{\partial z} + \frac{\partial w}{\partial y}\right) \\ \frac{1}{2}\left(\frac{\partial u}{\partial z} + \frac{\partial w}{\partial x}\right) & \frac{1}{2}\left(\frac{\partial v}{\partial z} + \frac{\partial w}{\partial y}\right) & \frac{\partial w}{\partial z} \end{bmatrix}$$

This relationship is of the form

$$\sigma_{ij} = K_{ijmn} e_{mn}$$

Since air is isotropic, the components of K must be the same in all Cartesian coordinate systems, therefore it can be shown that there are only two non zero components of K, λ and μ. The components of τ can now be written as

$$\tau_{ij} = -p\delta_{ij} + \lambda\delta_{ij}e_{mm} + 2\mu e_{ij}$$

Under the Stokes' hypothesis,$\lambda + \frac{2}{3}\mu = 0$ and the thermodynamic pressure is equivalent to the mechanical pressure. μ is the dynamic viscosity coefficient which is a friction coefficient. It is a function of temperature. The kinematic viscosity coefficient is defined to be $\nu = \mu/\rho$. The Navier-Stokes equations are given next in Cartesian coordinates where $\mathbf{r} = (x, y, z)$ so that $\mathbf{v} = (u, v, w) = (\frac{dx}{dt}, \frac{dy}{dt}, \frac{dz}{dt})$.

$$\begin{aligned}
&\frac{\partial \mathbf{v}}{\partial t} && \text{local derivative} \\
&+ (\mathbf{v} \cdot \nabla)\, \mathbf{v} && \text{nonlinear advection} \\
&= -\frac{1}{\rho}\nabla p && \text{pressure gradient force} \\
&+ \mathbf{g} && \text{gravity or other forces} \\
&+ \nu\nabla^2\mathbf{v} && \text{friction}
\end{aligned}$$

where

$$\nabla^2\mathbf{v} = \frac{\partial^2\mathbf{v}}{\partial x^2} + \frac{\partial^2\mathbf{v}}{\partial y^2} + \frac{\partial^2\mathbf{v}}{\partial z^2}$$

Other force terms can be added, such as buoyancy and Coriolis effects. The Navier-Stokes system consists of these three equation and an equation for conservation of mass. Since mass = density times volume, mass m can be expressed as

$$m = \int_V \rho \, \mathrm{d}V = \iiint \rho \, \mathrm{d}x \, \mathrm{d}y \, \mathrm{d}z$$

where V is a fixed volume. The rate of change of mass can be written as

$$\frac{dm}{dt} = \frac{d}{dt}\int_V \rho \, \mathrm{d}V = \int_V \frac{\partial \rho}{\partial t} \, \mathrm{d}V$$

Let A be the surface area of the boundary of V. The rate of mass flow out of the volume is

$$\int_A \rho \mathbf{v} \cdot \hat{n} \, \mathrm{d}A$$

where $\hat{n}$ is the unit normal vector that points out of the solid V. Using the two expressions for the rate of change of the mass and the divergence theorem gives

$$\int_V \frac{\partial \rho}{\partial t} \, \mathrm{d}V = -\int_A \rho \mathbf{v} \cdot \hat{n} \, \mathrm{d}A = -\int_V \nabla \cdot (\rho \mathbf{v}) \, \mathrm{d}V$$

Putting the left and right sides of the equation together

$$\int_V \left(\frac{\partial \rho}{\partial t} + \nabla \cdot (\rho \mathbf{v}) \right) \, \mathrm{d}V = 0$$

The volume V is fixed, but arbitrary, so the general equation for conservation of mass follows:

$$\frac{\partial \rho}{\partial t} + \nabla \cdot (\rho \mathbf{v}) = 0$$

The general form of conservation of mass is:

$$\frac{\partial \rho}{\partial t} + \nabla \cdot (\rho \mathbf{v}) = 0$$

If the density of air, ρ, is assumed to be constant then $\frac{\partial \rho}{\partial t} = 0$ and

$$\nabla \cdot (\rho \mathbf{v}) = \rho \, (\nabla \cdot \mathbf{v}) = 0$$

The fourth equation of the incompressible Navier-Stokes system is the incompressibility condition $\nabla \cdot \mathbf{v} = 0$

Let $\Omega \subseteq \mathbb{R}^3$ be a bounded domain. The stationary Navier-Stokes Equations are of the form:

$$
\begin{aligned}
&(\mathbf{v} \cdot \nabla)\, \mathbf{v} + \frac{1}{\rho} \nabla p - \nu \nabla^2 \mathbf{v} = \mathbf{g} \\
&\nabla \cdot \mathbf{v} = 0 \\
&\mathbf{v} = 0 \text{ on the boundary of } \Omega
\end{aligned}
$$

The weak formulation is given by:

$$
\begin{aligned}
&\nu \int_\Omega \nabla \mathbf{u} \nabla \mathbf{v}\ dx - \underbrace{\int_{\partial\Omega} (\nabla \mathbf{u} \cdot \mathbf{u}) \mathbf{v}\ ds}_{=0} + \int_\Omega (\mathbf{u} \cdot \nabla) \mathbf{u} \cdot \mathbf{v}\ dx \\
&\underbrace{- \int_\Omega p (\nabla \cdot \mathbf{v})\ dx}_{=0} + \underbrace{\int_{\partial\Omega} p \mathbf{v}\ ds}_{=0} = \int_\Omega f \mathbf{v}\ dx
\end{aligned}
$$

where $\mathbf{u}$ and $\mathbf{v}$ are in the space $[H_0^1(\Omega)]^3$ and f is in the space $L^2(\Omega)$

The following theorem is well known:

Theorem 2.1. *There exists a weak solution* $\mathbf{u}$ *of the Navier-Stokes Equations and a constant* $c_1 > 0$ *such that*

$$\|\mathbf{u}\|_{H^1} \leq \frac{c_1}{\nu} \|\mathbf{f}\|_{L^2}$$

Also, there exists a constant $c_2 = c_2(\Omega) > 0$*, such that the solution of the Navier-Stokes Equations is unique, if*

$$\nu^2 \geq c_2^2 \|\mathbf{f}\|_{L^2}$$

The symmetry of the system suggests using cylindrical coordinates. Consider a wind field in cylindrical coordinates (u, v, w) where u is the radial velocity, v is the tangential velocity and w is the vertical velocity of a parcel of air at location (r, θ, z). Under the assumptions of time independence, axisymmetry (no dependence on θ), pressure dependence only on r and z, and body force $b(r, z)$ due to buoyancy alone, the equations in cylindrical coordinates become:

1. The radial equation:

$$u\frac{\partial u}{\partial r} - \frac{v^2}{r} + w\frac{\partial u}{\partial z} = -\frac{1}{\rho}\frac{\partial p}{\partial r} + \nu\left(\frac{1}{r}\frac{\partial}{\partial r}\left(r\frac{\partial u}{\partial r}\right) - \frac{u}{r^2} + \frac{\partial^2 u}{\partial z^2}\right)$$

2. The tangential equation:

$$u\frac{\partial v}{\partial r} + \frac{uv}{r} + w\frac{\partial v}{\partial z} = \nu\left(\frac{1}{r}\frac{\partial}{\partial r}\left(r\frac{\partial v}{\partial r}\right) - \frac{v}{r^2} + \frac{\partial^2 v}{\partial z^2}\right)$$

3. The vertical equation:

$$u\frac{\partial w}{\partial r} + w\frac{\partial w}{\partial z} = -\frac{1}{\rho}\frac{\partial p}{\partial z} + \nu\left(\frac{1}{r}\frac{\partial}{\partial r}\left(r\frac{\partial w}{\partial r}\right) + \frac{\partial^2 w}{\partial z^2}\right)$$

4. Conservation of mass:

$$\frac{\partial u}{\partial r} + \frac{u}{r} + \frac{\partial w}{\partial z} = 0$$

2.3 Vorticity and Circulation

Vorticity is defined to be twice the average angular velocity of a fluid at a particular point of interest about each axis of an orthonormal coordinate system centered at the point of interest. In other words, vorticity is twice the local

angular velocity. Two mutually perpendicular lines are used and the average rotation rate of the two lines is calculated to get vorticity.

The vorticity vector $\mathbf{w}$. of a fluid element is related to the velocity vector $\mathbf{u}$ by $\mathbf{w} = \nabla \times \mathbf{u}$. Velocity $\mathbf{u}$ is related to circulation Γ around a closed contour C by

$$\Gamma \equiv \oint_C \mathbf{u} \cdot \mathbf{ds}$$

where $d\mathbf{s}$ is an element of contour C. By Stokes' Theorem,

$$\Gamma = \int_A \mathbf{w} \cdot \mathbf{dA}$$

where A is an arbitrary surface bounded by curve C. Thus, the circulation around a closed curve is equal to the surface integral of the vorticity. Equivalently, the vorticity at a point equals the circulation per unit area.

Chapter 3

Tangential Wind Models

The tangential component of the vortex wind is assumed known. The tangential wind profile is expressed as a product

$$v(r, z) = \phi(r)\psi(z)$$

where ϕ gives the radial profile of the tangential wind and ψ gives the vertical profile of the maximum tangential wind. The model for the function ψ is

$$\psi(z) = V_x \tanh\left(\frac{A_1 z}{H}\right) \tanh\left(A_2\left(1 - \frac{z}{H}\right)\right)$$

Where V_x is a parameter representing the maximum tangential velocity at the vertical level z. A_1, A_2 and H are parameters.

The function ϕ is normalized in the Wood-White and Vatistas models so that the maximum tangential wind is one at $r = 1$. The following is a list of candidate models for ϕ. There are three possible parameters and these will be denoted by a, b, and c. In order to simplify the form of the models, the symbols η and κ will be defined as $\eta = a + b$ and $\kappa = a + 1$.

1. The normalized Wood-White vortex 1.

$$\phi(r) = \frac{\kappa r}{a + r^{\kappa}}$$

2. The normalized Wood-White vortex 2.

$$\phi(r) = \frac{\eta r^b}{a + br^\eta}$$

3. The normalized Wood-White vortex 3.

$$\phi(r) = \frac{r^b}{\left[1 + \frac{b}{\eta}\left(r^{\frac{\eta}{c}} - 1\right)\right]^c}$$

4. The normalized Wood-White vortex 4

$$\Phi(r) = \frac{(rr_\star)^b + rr_\star}{1 + (rr_\star)^a} \Big/ \frac{(r_\star)^b + r_\star}{1 + (r_\star)^a}$$

where $r_\star$ is the radius where $\phi(r)$ is maximum.

5. The normalized Wood-White vortex 5

$$\Phi(r) = \frac{(rr_\star)^b + rr_\star}{\left(1 + (rr_\star)^{\frac{a}{c}}\right)^c} \Big/ \frac{(r_\star)^b + r_\star}{\left(1 + (r_\star)^{\frac{a}{c}}\right)^c}$$

where $r_\star$ is the radius where $\phi(r)$ is maximum.

For the Wood-White models, u, w, and pressure are computed using the Navier-Stokes equations. These computations are discussed later.

6. The Rankine combined vortex

$$u(r,\theta,z) = 0$$

$$v(r,\theta,z) = \begin{cases} \frac{V_x r}{R_x} & \text{if } r \leq R_x \\ \frac{V_x R_x}{r} & \text{if } r > R_x \end{cases}$$

$$w(r,\theta,z) = 0$$

where V_x is the maximum tangential velocity magnitude and R_x is the radius of the vortex core. $\frac{V_x}{R_x}$ is the angular velocity of the solid body rotation.

Since the angular momentum at infinity, Γ_∞ is

$$\lim_{r\to\infty} 2\pi r v = \Gamma_\infty,$$

then these equations can be written as

$$u(r,\theta,z) = 0$$

$$v(r,\theta,z) = \begin{cases} \frac{\Gamma_\infty r}{2\pi R_x^2} & \text{if } r \leq R_x \\ \frac{\Gamma_\infty}{2\pi r} & \text{if } r > R_x \end{cases}$$

$$w(r,\theta,z) = 0$$

In this model the vertical vorticity is given by

$$\zeta = \frac{\partial v}{\partial r} + \frac{v}{r} = \begin{cases} \frac{2V_x}{R_x} & \text{if } r \leq R_x \\ 0 & \text{if } r > R_x \end{cases}$$

Under the assumption of cyclostrophic balance, the perturbation pressure p' can be calculated by

$$\frac{\partial p'}{\partial r} = \frac{\rho v^2}{r} \tag{3.1}$$

To obtain the pressure, integrate (3.1) assuming p' is a function of r only.

$$\int_{p'(r)}^{p'_\infty} \mathrm{d}p = \int_r^\infty \frac{\rho v^2}{s}\, \mathrm{d}s$$

where $p'(r)$ is the pressure perturbation at radius r from the vortex center and p'_∞ is the pressure perturbation far away from the vortex. Under the assumption of constant density $p'_\infty = 0$. The pressure field for $r > R_x$ is

$$\begin{aligned} p'(r) &= -\int_r^\infty \rho \left(\frac{V_x R_x}{s}\right)^2 \frac{\mathrm{d}s}{s} \\ &= -\rho V_x^2 R_x^2 \left[-\frac{1}{2s^2}\right]_r^\infty = -\frac{1}{2}\rho V_x^2 \frac{R_x^2}{r^2} \end{aligned}$$

The pressure field for $r \le R_x$ is

$$\begin{aligned} p'(r) &= -\int_r^{R_x} \rho \left(\frac{V_x s}{R_x}\right)^2 \frac{\mathrm{d}s}{s} - \int_{R_x}^\infty \rho \left(\frac{V_x R_x}{s}\right)^2 \frac{\mathrm{d}s}{s} \\ &= -\frac{\rho V_x^2}{R_x^2}\left[\frac{s^2}{2}\right]_r^{R_x} - \rho V_x^2 R_x^2 \left[-\frac{1}{2s^2}\right]_{R_x}^\infty = -\rho V_x^2 \left(1 - \frac{r^2}{2R_x^2}\right) \end{aligned}$$

7. The Burgers-Rott vortex

$$u(r,\theta,z) = -ar$$
$$v(r,\theta,z) = \frac{\Gamma_\infty}{2\pi r}\left(1 - e^{-\frac{ar^2}{2\nu}}\right)$$
$$w(r,\theta,z) = 2az$$

where a is the strength of the suction, and Γ_∞ is

$$\lim_{r\to\infty} 2\pi r v = \Gamma_\infty,$$

Setting $\dfrac{\partial v}{\partial r} = 0$ gives maximum tangential winds when $\dfrac{1}{2\pi}\left(-\dfrac{1}{r^2} + \dfrac{1}{r^2}e^{-\frac{ar^2}{2\nu}} + \dfrac{a}{\nu}e^{-\frac{ar^2}{2\nu}}\right) = 0$

$$p(r,z) = p_0 + \rho\int_0^r \frac{v^2}{s}ds - \rho\frac{a^2}{2}\left(r^2 + 4z^2\right)$$

8. The normalized Vatistas vortex

$$\phi(r) = \frac{2^{\frac{1}{q}}r}{(1 + r^{2q})^{\frac{1}{q}}}$$

9. The Sullivan vortex

$$u(r) = -ar + \frac{6\nu}{r}\left(1 - e^{-\frac{ar^2}{2\nu}}\right)$$
$$v(r) = \frac{\Gamma_\infty}{2\pi H(\infty) r} H\left(\frac{ar^2}{2\nu}\right)$$
$$w(r) = 2az\left(1 - 3e^{-\frac{ar^2}{2\nu}}\right)$$

where $\Gamma_\infty = \lim_{R\to\infty} v(R) \cdot 2\pi R$ and

$$H(x) = \int_0^x exp\left[-\beta + 3\int_0^\beta (1 - e^{-s})\frac{1}{s} ds\right] d\beta$$

The vertical vorticity is computed as follows

$$\frac{\partial H(r)}{\partial r} = exp\left(-r + 3\int_0^r \frac{1 - e^{-s}}{s} ds\right)$$
$$\frac{\partial}{\partial r}\left(H\left(\frac{ar^2}{2\nu}\right)\right) =$$
$$\frac{ar}{\nu} exp\left(-\frac{ar^2}{2\nu} + 3\int_0^{\frac{ar^2}{2\nu}} \frac{1 - e^{-s}}{s} ds\right)$$
$$\zeta = \frac{\Gamma_\infty}{2\pi r H(\infty)} \frac{\partial}{\partial r}\left(H\left(\frac{ar^2}{2\nu}\right)\right)$$
$$\zeta = \frac{a\Gamma_\infty}{2\pi\nu H(\infty)} exp\left(-\frac{ar^2}{2\nu} + 3\int_0^{\frac{ar^2}{2\nu}} \frac{1 - e^{-s}}{s} ds\right)$$

The azimuthal vorticity for is given by the equation

$$\omega_\theta = \frac{\partial u}{\partial z} - \frac{\partial w}{\partial r} = \frac{-6a^2 rz}{\nu} e^{-\frac{ar^2}{2\nu}}$$

The pressure computations are as follows:

$$u\frac{\partial \Lambda}{\partial r} - \Lambda^2 - \nu\left(\frac{\partial^2 \Lambda}{\partial r^2} + \frac{1}{r}\frac{\partial \Lambda}{\partial r}\right) = -4a^2$$

$$p(r,z) = p_0 + \rho\int_0^r \frac{v^2}{s}ds - \rho\frac{a^2}{2}\left(r^2 + 4z^2\right) - \frac{18\rho\nu^2}{r^2}\left(1 - e^{-\frac{ar^2}{2\nu}}\right)^2$$

10. The double exponential vortex

$$\phi(r) = ae^{-bx} - ce^{-dx}$$

Chapter 4

The Data Set

Tornado wind data were generated by Davies-Jones (2007) [11], using a numerical model of a mesocyclone. Davies-Jones defined a mesocyclone as a cyclonic vortex with core radius greater then 2 km. The numerical model uses non-dimensional equations to solve for radial u, tangential v and vertical w winds with an initial Beltrami flow. The equations and numerical procedures are described in [11]. The independent variables, radius from the center r and height above the ground z were divided into an unstaggered grid with grid spacing $\Delta r = \Delta z = 42.25$ m when scaled to the mesocyclone. The portion of the data set used in this paper is from a snapshot of the simulation at $t = 6.07$ when the tornado produced by the mesocyclone is at its peak. The tornado regions occupies r_i, $i = 1, \cdots N_d$ with $N_d = 30$ and height $z = 1$, 2, and 3 levels from the ground. The variable r_i represents the distance from the vortex center and each height level corresponds to 42 m, 84 m and 126 m. Vertical and tangential winds in the axial jet reach speeds of 3.49 (119 m/s) and 2.27 (77 m/s), respectively. The tangential wind profile from the Davies-Jones data set was normalized to fit the Wood-White 2 vortex tangential wind model so that the maximum was one at the location $r = 1$ from the center of the tornado vortex. at this point, the data is non-dimensional. The maximum velocity was retained and used in the vertical wind profile of the horizontal maximum tangential wind for use in the z-dependent profile.

The Davies-Jones data set used in this paper was provided by Vincent T. Wood of NOAA/OAR/National Severe Storms Laboratory. The data is described fully in Davies-Jones [11].

Chapter 5

The Forward Problem

The prediction problem is called the forward problem. Let $\mathfrak{S}$ be the physical system under study. In this paper, $\mathfrak{S}$ is an atmospheric vortex. The non-linear model in $\mathfrak{S}$ is defined by $Y_{mn} = v(r_n, z_m, \mathbf{Q}) + \epsilon_{mn}$, $n = 1, 2, \ldots, N$, $m = 1, 2, 3$, where N is the number of independent variables that represent distance r from the vortex center and m defines the three levels that represent height z above the ground. The variable v is the tangential velocity and $\mathbf{Q} = (\mathbf{p}, \mathbf{q})$ is the vector of parameters with vector $\mathbf{p}$ containing parameters for the model of the tangential profile viewed radially from the vortex center and vector $\mathbf{q}$ containing parameters for the maximum tangential wind profile viewed vertically from the ground. It is assumed that

$$v(r_n, z_m, \mathbf{Q}) = \phi(r_n, \mathbf{p})\psi(z_m, \mathbf{q}) \tag{5.1}$$

The variable ϵ_{mn} is the random variable representing the stochastic or disturbance part of the model with $E(\epsilon_{mn}) = 0$ and $Var(\epsilon_{mn}) = \sigma^2$. Here σ^2 is assumed to be constant.

The physical laws and approximations applied to $\mathfrak{S}$ result in the Navier-Stokes equations. The form of the tangential velocity model is assumed known and given, both in the radial direction and the vertical direction. Hence, the form of the functions $\phi(r_n, \mathbf{p})$ and $\psi(z_m, \mathbf{q})$ are assumed known and given. Another assumption is that the independent variables r_n and z_m are known

without error.

A subset of the Navier-Stokes equations is used to estimate radial and vertical wind profiles. The question arises as to the accuracy of these predicted values. The uncertainty analysis for these predictions is described in the next section which focuses on the inverse problem. For the forward problem, two cases are considered. The first case is the Cylindrical Case where

$$\psi(z, \mathbf{q}) \equiv 1$$

In other words, the atmospheric vortex is a cylinder with no vertical variation. The second case is the Non-Cylindrical Case where

$$\psi(z, \mathbf{q}) = V_x \tanh\left(\frac{A_1 z}{H}\right) \tanh\left(A_2\left(1 - \frac{z}{H}\right)\right)$$

V_x is a parameter representing the maximum tangential velocity at the vertical level z and A_1, A_2, H are parameters.

5.1 Cylindrical Case

The tangential velocity is assumed to be a function of r only. In this cylindrical case, the vertical vorticity is given by

$$\zeta = \frac{\partial v}{\partial r} + \frac{v}{r} = \frac{\partial \phi}{\partial r} + \frac{\phi}{r}$$

Therefore, the vertical vorticity ζ is a function of r only. The tangential momentum equation becomes

$$u\frac{\partial \phi}{\partial r} + \frac{u\phi}{r} = \nu\left(\frac{\partial}{\partial r}\left(\frac{1}{r}\frac{\partial}{\partial r}(r\phi)\right)\right)$$
$$u\zeta = \nu\left(\frac{\partial \zeta}{\partial r}\right), r > 0$$

and this gives a solution for u given by

$$u = \nu\left(\frac{\frac{\partial \zeta}{\partial r}}{\zeta}\right), \zeta \neq 0 \tag{5.2}$$

Therefore, the radial velocity u is a function of r only.

Using the conservation of mass equation, the vertical velocity w is found by

$$\frac{\partial w}{\partial z} = -\left(\frac{\partial u}{\partial r} + \frac{u}{r}\right)$$
$$w = -\left(\frac{\partial u}{\partial r} + \frac{u}{r}\right)z \tag{5.3}$$

The radial momentum equation can be used to compute pressure.

Let $\Lambda = \frac{\partial u}{\partial r} + \frac{u}{r}$ so that $w = -z\Lambda$, since

$$w = -\left(\frac{\partial u}{\partial r} + \frac{u}{r}\right)z$$
$$u\frac{\partial u}{\partial r} - \frac{v^2}{r} = -\frac{1}{\rho}\frac{\partial p}{\partial r} + \nu\left(\frac{\partial}{\partial r}\left(\frac{1}{r}\frac{\partial}{\partial r}(ru)\right)\right)$$

which can be seen to be

$$u\frac{\partial u}{\partial r} - \frac{v^2}{r} = -\frac{1}{\rho}\frac{\partial p}{\partial r} + \nu\left(\frac{\partial \Lambda}{\partial r}\right)$$

so that

$$\frac{\partial p}{\partial r} = \rho\left(-u\frac{\partial u}{\partial r} + \frac{v^2}{r} + \nu\left(\frac{\partial \Lambda}{\partial r}\right)\right)$$

Solving this differential equation gives

$$p(r,z) = \rho\left(-u^2/2 + \int_0^r \frac{v^2}{s}ds + \nu\Lambda\right) + f(z)$$

where the function f is a function of z only.

The vertical equation gives

$$\frac{\partial p}{\partial z} = \rho z\left[u\frac{\partial \Lambda}{\partial r} - \Lambda^2 + \nu\left(\frac{1}{r}\frac{\partial}{\partial r}\left(r\frac{\partial \Lambda}{\partial r}\right)\right)\right]$$

Solving this differential equation gives

$$p(r,z) = \rho\frac{z^2}{2}\left[u\frac{\partial \Lambda}{\partial r} - \Lambda^2 + \nu\left(\frac{1}{r}\frac{\partial}{\partial r}\left(r\frac{\partial \Lambda}{\partial r}\right)\right)\right] + g(r)$$

where the function g is a function of r only. These two expressions for $p(r,z)$ must hold simultaneously.

5.2 NonCylindrical Case

In this noncylindrical case, the vertical vorticity is given by

$$\zeta = \frac{\partial v}{\partial r} + \frac{v}{r} = \left(\frac{\partial \phi}{\partial r} + \frac{\phi}{r}\right)\psi$$

where ϕ is a function of r only and ψ is a function of z only. The tangential momentum equation becomes $\zeta u + \eta w = \beta$

where $\eta(r,z) = \phi(r)\psi_z(z) = \phi\psi_z$ and $\beta(r,z) = \nu(\zeta_r(r,z) + \phi(r)\psi_{zz}(z)) = \nu(\zeta_r + \eta_z)$ Notice that $\eta \neq 0$ except at the z_0 level of maximum tangential velocity, in other words, where $\psi_z(z_0) = 0$ because $\phi(r) \neq 0$ only at $r = 0$. Solve the tangential equation for w and substitute this into the equation for conservation of mass:

$$w = \frac{\beta}{\eta} - \frac{\zeta u}{\eta} \tag{5.4}$$
$$\frac{\partial u}{\partial r} + \frac{u}{r} + \frac{\partial}{\partial z}\left[\frac{\beta}{\eta} - \frac{\zeta u}{\eta}\right] = 0$$

A first order partial differential equation in u follows as:

$$\frac{\partial u}{\partial r} - \frac{\zeta}{\eta}\frac{\partial u}{\partial z} + u\left[\frac{1}{r} + \frac{\zeta\eta_z}{\eta^2} - \frac{\zeta_z}{\eta}\right] + \frac{\beta_z}{\eta} - \frac{\beta\eta_z}{\eta^2} = 0$$
$$u(0, z) = 0$$

The method of characteristics was used to solve this partial differential equation by choosing $\frac{dr}{dt} = 1$ and $\frac{dz}{dt} = \frac{-\zeta}{\eta}$ so that $\frac{du}{dt} = \frac{du}{dr}(1) + \frac{du}{dz}\left(\frac{-\zeta}{\eta}\right)$ to get the ordinary differential equation:

$$\frac{\partial u}{\partial t} + u\left[\frac{1}{r} + \frac{\zeta\eta_z}{\eta^2} - \frac{\zeta_z}{\eta}\right] + \frac{\beta_z}{\eta} - \frac{\beta\eta_z}{\eta^2} = 0$$
$$u(0, z) = 0$$

Let $t = r$ and let s be the characteristic curve $s = r\phi\psi = t\phi\psi = tv$ Recall that $t\phi(r)\psi(z) = tv$ so that at a particular level, $\phi(t)\psi(z_0) = v(t, z_0)$ at $z = z_0$. Let

$$\eta = \phi\psi_z$$

$$\eta_z = \phi\psi_{zz}$$

$$\zeta = \left(\frac{\phi}{t} + \phi_t\right)\psi$$

$$\zeta_z = \left(\frac{\phi}{t} + \phi_t\right)\psi_z$$

$$\beta = \nu\left[\left(\phi_{tt} + \frac{\phi_t}{t} - \frac{\phi}{t^2}\right)\psi + \phi\psi_{zz}\right]$$

$$\beta_z = \nu\left[\left(\phi_{tt} + \frac{\phi_t}{t} - \frac{\phi}{t^2}\right)\psi_z + \phi\psi_{zzz}\right]$$

The coefficient of u becomes:

$$\left[\left(\frac{1}{t} + \frac{\phi_t}{\phi}\right)\frac{\psi\psi_{zz}}{\psi_z^2} - \frac{\phi_t}{\phi}\right]$$

The remaining term, $\frac{\beta_z}{\eta} - \frac{\beta\eta_z}{\eta^2}$ can be seen to be:

$$\nu\left[\left(\frac{\phi_{tt}}{\phi} + \frac{\phi_t}{t\phi} - \frac{1}{t^2}\right)\left(1 - \frac{\psi\psi_{zz}}{\psi_z^2}\right) + \frac{\psi_{zzz}}{\psi_z} - \frac{\psi_{zz}^2}{\psi_z^2}\right]$$

Therefore, the problem becomes to solve the ordinary differential equation given by:

$$\begin{aligned} u'(t) = f(t,u) &= \left[\frac{\phi_t}{\phi} - \left(\frac{1}{t} + \frac{\phi_t}{\phi}\right)\frac{\psi\psi_{zz}}{\psi_z^2}\right]u \\ &+ \nu\left[\left(\frac{\phi_{tt}}{\phi} + \frac{\phi_t}{t\phi} - \frac{1}{t^2}\right)\left(\frac{\psi\psi_{zz}}{\psi_z^2} - 1\right) - \frac{\psi_{zzz}}{\psi_z} + \frac{\psi_{zz}^2}{\psi_z^2}\right] \\ u(0) &= 0 \end{aligned} \tag{5.5}$$

The derivatives of ψ are given in Appendix A. The Euler method was used

to solve (5.5). The solution is unstable near $t = 0$ because the coefficients have terms involving $1/t$. It was necessary to solve (5.5) away from $t = 0$ by providing an initial condition $u(r_0)$ where $r_0 \neq 0$. This is equivalent to receiving one radial measurement to initialize (5.5). Once radial u is determined, vertical w can be calculated from the equation for conservation of mass.

Chapter 6

The Inverse Problem

The problem of using the results of some measurements to infer information on values of model parameters is called the inverse problem. In the system $\mathfrak{S}$ of an atmospheric vortex the tangential wind profile is assumed to be of the form $v(r, z, \mathbf{Q}) = \phi(r, \mathbf{p})\psi(z, \mathbf{q})$ (5.1), where $\mathbf{Q} = (\mathbf{p}, \mathbf{q})$ is the vector of parameters. It is assumed that each parameter is contained in a bounded interval of real numbers. The space of admissible parameters is defined as the Cartesian product of the bounded intervals of the parameters and hence is a bounded hypercube in $\mathbb{R}^{N_p}$, where N_p is the number of parameters. The solution of the inverse problem may be expressed in terms of a probability distribution over the space of admissible parameters. The probabilistic formulation of the inverse problem results in a collection of models, forming a model space, defined over the parameter space. Data is used to construct a probability density function (p.d.f.) over the parameter space which is then used to define a p.d.f. over the model space, Hence, the parameter estimation procedure provides a probability for each parameter vector in the parameter space from which an optimal parameter vector can be selected as the one with the highest probability. The parameter vector probability assigns to each model in the model space, a probability that the model is consistent with the data. A description of the parameter estimation procedure that will define this probability distribution is given below.

6.1 Z-Dependent Profile Parameters

The vertical profile of the maximum tangential wind, ψ is

$$\psi(z) = V_x \tanh\left(\frac{A_1 z}{H}\right) \tanh\left(A_2\left(1 - \frac{z}{H}\right)\right)$$

where V_x is a parameter representing the maximum tangential velocity at the vertical level z. A_1, A_2 and H are parameters. These parameters are estimated using a data set of maximum tangential wind profiles by minimizing the cost functional over the admissible set of parameters:

$$J(\mathbf{q}) = \sum_{i=1}^{N} \left(\psi(z_i, \mathbf{q}) - \psi_{obs}(z_i)\right)^2$$

where $\mathbf{q}$ is the vector of parameters with components q_k, $k = 1, \cdots, N_q$. In this case, $q_1 = V_x$, $q_2 = A_1$, $q_3 = A_2$ and $q_4 = H$ with $N_q = 4$ and $1 \leq z \leq 15$. The function $\psi_{obs}(z_i)$ is the maximum tangential velocity at each level of z_i.

At this time, the only data set with more than one vertical level available for this analysis is the Davies-Jones data set. Future work will include other data sets. The z-profile model is fitted to the Davies-Jones maximum tangential velocity data by minimizing $J(\mathbf{q})$ using $0.3 \leq V_x \leq 3$, $1 \leq A_1 \leq 6$, $1 \leq A_2 \leq 6$ and $16 \leq H \leq 46$. The optimal parameter values of $\hat{q}_1 = \hat{V}_x = 2.8$, $\hat{q}_2 = \hat{A}_1 = 3.9$, $\hat{q}_3 = \hat{A}_2 = 2.2$, and $\hat{q}_4 = \hat{H} = 30$ with $J(\mathbf{q}) = 0.001351$ using grid spacing of 0.1 for each of the parameters V_x, A_1, and A_2 and grid spacing of one for H. Note that V_x, A_1, and A_2 are assumed to be real numbers and H is assumed to be an integer. Figure 6.1 shows the z-profile fitted to the Davies-Jones maximum tangential velocity data.

The parameters and the functional form of the z-dependent profile are dependent on the type of atmospheric vortex and will not be a part of the uncer-

Figure 6.1: z-Profile fitted to Davies-Jones

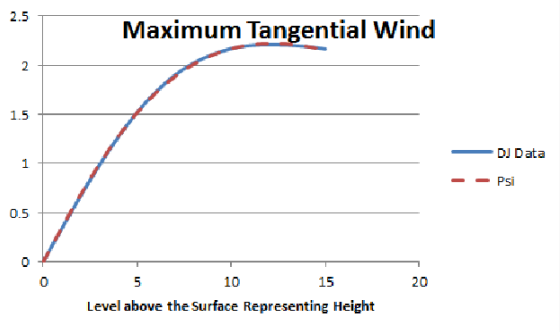

tainty analysis. Therefore, these parameters are estimated and assumed to be accurate.

6.2 Tangential Profile Parameters

Since the estimated z-dependent parameters are assumed to be accurate, the non-linear regression model can be simplified and written as $Y_n = \phi(r_n, \mathbf{p}) + \epsilon_n$ where ϵ_n is the random variable representing the stochastic or disturbance part of the model and is assumed normally distributed with $E(\epsilon_n) = 0$ and $Var(\epsilon_n) = \sigma^2$, a constant. Parameters were estimated by minimizing the objective or cost function:

$$J(\mathbf{p}) = \sum_{i=1}^{N} \left(\phi(r_i, \mathbf{p}) - \phi_{obs}(r_i)\right)^2 = \sum_{i=1}^{N} \left(\phi(r_i, \mathbf{p}) - z_i\right)^2$$

where $\mathbf{p}$ is the vector of parameters with components p_k, $k = 1, \cdots, N_p$, r_i is distance from the center of the vortex and assumed known without error. All model parameters were estimated using a grid on each parameter interval with spacing size 0.01 and by the following steepest descent algorithm:

1. The first estimate $\mathbf{p_0}$ is selected by using a grid over the admissible pa-

rameters with spacing 0.1. $\mathbf{p_0}$ is chosen so that $J(\mathbf{p})$ is minimized over the grid.

2. Calculate the derivative

$$DJ(\mathbf{p}) = \sum_{i=1}^{N} \left(\phi(r_i, \mathbf{p}) - \phi_{obs}(r_i)\right) D_{\mathbf{p}}\phi(r_i, \mathbf{p})$$

3. Select s and calculate

$$\mathbf{p}(s) = \mathbf{p_0} - s\frac{DJ(\mathbf{p})}{||DJ(\mathbf{p})||}$$

   Now select the largest s^* so that $J(\mathbf{p}(s))$ decreases.

4. Let $\mathbf{p_0} = \mathbf{p}(\mathbf{s}^*)$ and continue the process until the sequence converges. The sequence can converge since $J(\mathbf{p})$ and $DJ(\mathbf{p})$ are continuous. There is no assumption of convergence to a unique point.

In the objective function, the quantity $d_i = \phi(r_i, \mathbf{p}) - z_i$ for $i = 1, 2, \ldots, N$ is called the residual. The assumptions on the residuals are as follows:

1. The residuals are independently distributed. This means that the residuals are independent of one another.

2. Each residual is normally distributed. This is important because it is an underlying assumption that non-linear least squares will lead to a maximum likelihood estimate.

3. Each residual has zero mean. This assumption can be relaxed by adding a bias term to the expectation function.

4. Residuals have equal variances. The main implication of this assumption is that all residuals are equally unreliable so that the least squares criterion can be used.

The Runs Test and the Correlated Residuals Test can be used to test the first assumption. The remaining assumptions can be tested using the Normality Tests. These tests are all described in this chapter.

6.3 Determination of the Parameter ν

Parameter ν was estimated by selecting 10000 random values from the interval $[0, 1]$ assuming a uniform distribution for ν in this interval. For each selected ν, the Euler method was used to solve equation (5.5) for u. The objective function

$$J(\nu) = \sum_{i=1}^{N} \left(u(r_i, \nu) - u_{obs}(r_i)\right)^2$$

was minimized and the optimal value for ν was obtained. A value $\nu = 0.102$ was selected to use for all z levels under consideration.

6.4 Analysis of the Residuals

Define the residuals $d(r_i) = \phi(r_i, \hat{\mathbf{p}}) - \phi_{obs}(r_i) = \phi(r_i, \hat{\mathbf{p}}) - z_i$ for $i = 1, \cdots N_d$. Each residual is thus an estimate of the disturbance ϵ_n.The mean and standard deviation of the residuals are computed by:

$$\mu_R = \sum_{i=1}^{N} d(r_i)/N \qquad\qquad \sigma_R = \sqrt{\sum_{i=1}^{N} d(r_i)^2/(N-1)}$$

6.4.1 Runs Test

A runs test is used to test for randomness. The following information can be found in Gibbons [12]. This test determines whether the curve deviates systematically from the data. A run is a series of consecutive points that are either all above or all below the regression curve. A sequence is considered non-random if there are either too many or too few runs, and random otherwise. Let n_1 be the number of points above the regression curve, n_2 be the number of points below the regression curve and n be the total number of points so that $n = n_1 + n_2$. Let r_1 be the number of runs consisting of points above the regression curve and let r_2 be the number of runs consisting of points below the regression curve with r the total number of runs so that $r = r_1 + r_2$. Let R be the random variable representing the number of runs.

Theorem 6.1. *The probability distribution of R, the total number of runs of* $n = n_1 + n_2$ *objects,* n_1 *of type 1 and* n_2 *of type 2, in a random sample is*

$$f_R(r) = \begin{cases} 2\dfrac{\binom{n_1-1}{r/2-1}\binom{n_2-1}{r/2-1}}{\binom{n_1+n_2}{n_1}} & \text{if } r \text{ is even, else} \\ \dfrac{\binom{n_1-1}{(r-1)/2}\binom{n_2-1}{(r-3)/2}+\binom{n_1-1}{(r-3)/2}\binom{n_2-1}{(r-1)/2}}{\binom{n_1+n_2}{n_1}} & \end{cases}$$

for $r = 2, 3, \cdots, n_1 + n_2$

The probability distribution $f_R(r)$ can be used to test the hypothesis of randomness if $n_1 + n_2 \leq 20$. For larger sample sizes, it is more convenient to use the mean and variance of this distribution creating a z-statistic to compare to the normal distribution. The mean and variance of this distribution are given by:

$$\mu_R = \frac{2N_1N_2}{N_1 + N_2} + 1$$
$$\sigma_R^2 = \frac{2N_1N_2(2N_1N_2 - N_1 - N_2)}{(N_1 + N_2)^2(N_1 + N_2 - 1)}$$

The hypothesis of randomness is tested with the z- statistic: $z = \frac{R-\mu_R}{\sigma_R}$. This statistic is normally distributed with mean 0 and variance 1.

6.4.2 Correlated Residuals

The tangential wind profile has distance from the vortex center as the independent variable, therefore if the condition of independence of residuals is not met, correlation of the residuals should be investigated. Since the data are equally spaced in distance from the vortex center, a plot of the residual autocorrelation function versus the lag k can provide information about the correlation between the residuals. This autocorrelation function is calculated by [2]:

$$r_k = \sum_{i=k+1}^{N} \frac{d(r_i)d(r_{i-k})}{Ns^2}$$

where s^2 is the variance estimate and the residuals are assumed to have zero mean. If the residual autocorrelation function is consistently within the range $\pm 2/\sqrt{N}$ after lag 2 or 3, then the model may be identified as a moving average process of order 1 or 2. If the residual autocorrelation function tends to

decay gradually to zero, then the process may be identified as an autoregressive process.

6.4.3 Normality Tests

Measures of Variance, Skewness and Kurtosis

The following information can be found in Roussas [21].

Definition 6.2 (Central Moments about the Mean)**.** Let X be a random variable with mean μ. The rth central moment of X about μ is defined by $\mu_r = E(X-\mu)^r$. The mean of the random variable X is defined to be $\mu = E(X)$.

The second central moment about the mean is the population variance σ^2.

Definition 6.3 (Coefficient of Skewness)**.** Let X be a random variable with mean μ and finite third central moment about the mean. The skewness of the distribution of the random variable X is defined by the dimensionless quantity

$$S_k = E\left(\frac{X-\mu}{\sigma}\right)^3$$

The skewness of the distribution of the random variable X is a measure of the asymmetry of the distribution. If $S_k > 0$, the distribution is said to be skewed to the right and if $S_k < 0$, the distribution is said to be skewed to the left. If the p.d.f. of X is symmetric about μ, then $S_k = 0$, as is the case for the Normal distribution.

Definition 6.4 (Coefficient of Kurtosis)**.** Let X be a random variable with mean μ and finite fourth central moment about the mean. The kurtosis of the distribution of the random variable X is defined by the dimensionless quantity

$$K = E\left(\frac{X-\mu}{\sigma}\right)^4 - 3$$

The kurtosis of the distribution is a measure of "peakedness" of the distribution compared to the Normal distribution with mean zero and variance equal to one as a reference. The fourth central moment of this reference normal distribution is equal to three. If $K > 0$, the distribution is called leptokurtic and if $K < 0$, the distribution is called platykurtic. If $K = 0$ and the distribution has the same "peakedness" as the normal distribution, then the distribution is called mesokurtic.

Definition 6.5 (Sample Central Moments about the Mean)**.** Let $X_1, X_2, \cdots X_n$ be a random sample of identically distributed random variables with sample mean $\bar{X}$. The rth sample central moment of the sample is defined by

$$m_r = \frac{\sum_{i=1}^{n}(X_i - \bar{X})^r}{n}$$

The second sample central moment about the mean is the sample variance s^2.

Definition 6.6 (Unbiased Sample Variance)**.** Let $X_1, X_2, \cdots X_n$ be a random sample of identically distributed random variables with sample mean $\bar{X}$. The unbiased estimator of the variance is

$$\hat{s}^2 = \frac{n-1}{n}s^2$$

Definition 6.7 (Sample Coefficient of Skewness)**.** Let $X_1, X_2, \cdots X_n$ be a random sample of identically distributed random variables with sample mean $\bar{X}$. The sample skewness of the distribution of the random variable X is

$$s_k = \frac{m_3}{\left(\sqrt{m_2}\right)^3} = \frac{\sum_{i=1}^{n}(X_i - \bar{X})^3/n}{\left(s\sqrt{(n-1)/n}\right)^3}$$

Definition 6.8 (Unbiased Sample Coefficient of Skewness)**.** Let $X_1, X_2, \cdots X_n$ be a random sample of identically distributed random variables with sample mean $\bar{X}$. The unbiased estimator of the coefficient of skewness is

$$\hat{s}_k = \frac{\sqrt{n(n-1)}}{n-2} s_k$$

Definition 6.9 (Sample Coefficient of Kurtosis)**.** Let $X_1, X_2, \cdots X_n$ be a random sample of identically distributed random variables with sample mean $\bar{X}$. The sample skewness of the distribution of the random variable X is

$$K = \frac{m_4}{(m_2)^2} = \frac{\sum_{i=1}^{n}(X_i - \bar{X})^4/n}{(s^2(n-1)/n)^2}$$

The excess of Kurtosis is defined to be the difference between the sample kurtosis and the kurtosis of a normal distribution. The kurtosis of a normal distribution is equal to 3.

Definition 6.10 (Unbiased Sample Estimator of the Excess of Kurtosis)**.** Let $X_1, X_2, \cdots X_n$ be a random sample of identically distributed random variables with sample mean $\bar{X}$. The unbiased estimator of the excess of Kurtosis is

$$\hat{K} = \frac{(n+1)(n-1)}{(n-2)(n-3)} \left(K - \frac{3(n-1)}{n+1} \right)$$

The Jarque-Bera test for normality [14] is used to test the following hypothesis:

H_0 : The data comes from a normal distribution with skewness = 0 and Kurtosis = 3.

H_1 : The data is not from a normal distribution.

The test statistic is given by:

$$JB = \frac{N}{6}\left(\hat{s}_k + \frac{(\hat{K})^2}{4}\right)$$

This has a Chi-Square distribution with 2 degrees of freedom under the assumption that the mean of the data is zero.

Kolmogorov-Smirnov Normality Test

The following information can be found in Gibbons [12].

An important question in statistics concerns the form of the population from which a sample is drawn. Suppose a random sample of size N is drawn from a population with unknown c.d.f. F_Z. It is of interest to test whether F_Z is equal to some completely specified c.d.f. $F_0(z)$. Let $Z_1, Z_2, \cdots Z_N$ be a random sample from a distribution F_Z. For example, Z_i could be a normalized residual, $z_i = \frac{d(r_i)-\mu}{\sigma}$, $i = 1, 2, \cdots N$ where $d(r_i) = \phi(r_i, \hat{\mathbf{p}}) - \phi_{obs}(r_i)$ for $i = 1, \cdots N_d$. The empirical (sample) distribution function of this random sample, $F_N(z)$ can be calculated by:

$$F_N(z) = \frac{1}{N}[\text{the number of } z_i \leq z]$$

Thus F_N is a step function which increases by the amount $1/N$ at its jump points. The jump points are the order statistics of the sample, $Z_{(1)}$, $Z_{(2)}$, $\cdots$

$Z_{(N)}$. The empirical distribution can now be defined as:

$$f_N(z) = \begin{cases} 0 & \text{if } z < X_{(1)} \\ \frac{k}{N} & \text{if } X_{(k)} < z < X_{(k+1)} \quad \text{for } k = 1, 2, \cdots, N-1 \\ 1 & \text{if } z \geq X_{(N)} \end{cases}$$

For a fixed value of z, $F_N(z)$ is a random variable and therefore has a probability density function.

Theorem 6.11. *For the random variable $F_N(z)$, which is the empirical distribution function of a random sample $Z_1, Z_2, \cdots, Z_N$ from a distribution F_Z, then*

$$P\left[F_N(z) = \frac{j}{N}\right] = \begin{pmatrix} N \\ j \end{pmatrix} [F_Z(z)]^j [1 - F_Z(z)]^{N-j}, \ j = 0, 1, \cdots, N$$

with mean and variance given by:

$$E[F_N(z)] = F_Z(z)$$
$$var[F_N(z)] = \frac{F_Z(z)[1 - F_Z(z)]}{N}$$

The above theorem shows that $F_N(z)$ is an unbiased estimator of $F_Z(z)$, and from the law of large numbers that $F_N(z)$ is a consistent estimator of $F_Z(z)$, in other words, $F_N(z)$ converges in probability to $F_Z(z)$. A stronger result can be obtained and is given in the next theorem.

Theorem 6.12 (Glivenko-Cantelli Theorem)**.** *$F_N(z)$ converges uniformly to*

F_Z with probability one; that is,

$$P[\lim_{N\to\infty} \sup_{-\infty<z<\infty} |F_Z(z) - F_N(z)| = 0] = 1$$

As a result of the Glivenko-Cantelli Theorem, since the convergence is uniform, the deviations between $F_N(z)$ and $F_Z(z)$ should be small for all values of z for large N. Thus the Kolmogorov-Smirnov one-sample statistic given by:

$$D_N = \sup_z |F_Z(z) - F_N(z)|$$

should be a reasonable measure of the accuracy of the estimate. The Kolmogorov-Smirnov one-sample statistic can be used to test the hypothesis: $H_0 : F_Z(z) = F_0(z)$ for all z against the alternative $H_1 : F_Z(z) \neq F_0(z)$ for some z. The statistic can also be used to find confidence bands for $F_Z(z)$ for all z. Using the probability density function for the statistic D_N, the number $D_{N,\alpha}$ can be found so that for any probability $1 - \alpha$,

$$P[F_N(z) - D_{N,\alpha} < F_Z(z) < F_N(z) + D_{N,\alpha}] = 1 - \alpha$$

Since $0 \leq F_Z(z) \leq 1$ for all z, then the numbers $L_N(z) = max[F_N(z) - D_{N,\alpha}, 0]$ and $U_N(z) = min[F_N(z) + D_{N,\alpha}, 1]$ define a confidence band for $F_Z(z)$, with associated confidence coefficient $1 - \alpha$. Both the hypothesis test and the confidence band require knowledge of a probability distribution function for the statistic D_N. Gibbons [12] gives the p.d.f. for D_N when the parameters of the continuous distribution $F_0(z)$ are completely specified. In the case that $F_0(z)$ is a normal distribution with mean and variance that must be estimated from the data, Lilliefors [16] provides a table for use with the Kolmogorov-Smirnov one-sample statistic. The table is obtained from a Monte-Carlo calculation.

6.5 Probability Distributions

Two types of joint and marginal probability distributions are considered for the parameters $\mathbf{p}$. The first type is the uniform probability distribution under the assumption of no prior information except for bounds on the values of the parameters. The second type is a quasi-normal distribution defined by $f(\mathbf{p}) = C\exp(-J(\mathbf{p}))$. The real number C results so that the volume under the surface is one, thus creating a probability distribution function (p.d.f). The parameters are from a closed and bounded subset of $\mathbb{R}^{N_p}$, where N_p is the number of parameters. A marginal distribution function for a single parameter can be calculated by integrating over the domain of the remaining parameters.

The mean $E(X)$ and variance σ_X^2 of a random variable X were defined in section 6.4. Covariance and correlation are defined now:

Definition 6.13 (Covariance and Correlation)**.** Let X be a random variable with mean $E(X)$ and variance σ_X^2. Let Y be a random variable with mean $E(Y)$ and variance σ_Y^2. Then the covariance, $cov(X,Y)$, and correlation $r(X,Y)$ are defined to be:

$$cov(X,Y) = E\{[X - E(X)][Y - E(Y)]\} \tag{6.1}$$

$$r(X,Y) = \frac{cov(X,Y)}{\sigma_X \sigma_Y} \tag{6.2}$$

The mean and variance of each parameter along with the covariance and correlation between parameters can be calculated from the probability distribution and cumulative distribution functions. Therefore, the uniform p.d.f. and the p.d.f. determined from the benchmark data can be used to quantify the

uncertainty in the parameters. The probability distributions will be defined in three ways:

1. A Uniform distribution over the space of admissible parameters under the assumption of no prior knowledge of the parameters except for lower and upper bounds.

2. A Normal distribution over each parameter with assumptions on the value of the mean and standard deviation given by physical properties of the vortex.

3. A probability distribution defined by a benchmark data set. Here benchmark data set is defined to be a data set that is believed to be accurate and true for use in comparing information with computational results and for drawing conclusions from these comparisons.

Random samples from these distributions are used in uncertainty analysis and model selection. The next section describes the types of random samples used in this atmospheric vortex data analysis.

6.6 Random Samples

6.6.1 Sample from a Grid

Samples from a grid are not random and can be used to compare samples gathered by another method. It is assumed that each parameter is from a closed and bounded interval in $\mathbb{R}$. The interval is divided into equally spaced subintervals of length h. This defines a finite grid over the space of admissible parameters. If there are many parameters, the size of the sample obtained in this manner can be quite large. The underlying probability distribution can be calculated as uniform by $f(\mathbf{p}) = 1/M$, where M is the number of points

in the grid. The underlying probability distribution can be calculated using a benchmark data set over the grid points using the p,d.f. with normalizing constant C $f(\mathbf{p}) = C\exp(-J(\mathbf{p}))$.

6.6.2 Gibbs Sample

A Gibbs sample can be collected from the sample from a grid. The procedure will be given using two parameters a and b as follows:

1. The first point in the Gibbs sample is selected to be $a[0] = \hat{a}$ and $b[0] = \hat{b}$. Selection of this point is arbitrary.

2. The pdf $f(a|b = b[i-1])$ is obtained from the joint pdf calculated above.

3. The cumulative probability distribution cdf $F(a|b = b[i-1])$ is generated from $f(a|b = b[i-1])$.

4. A random number r was generated from a uniform distribution $U[0,1]$. This random number and the cdf $F(a|b = b[i-1])$ gives $a[i]$.

5. The pdf $f(b|a = a[i])$ is obtained from the joint pdf calculated above.

6. The cumulative probability distribution cdf $F(b|a = a[i])$ is generated from $f(b|a = a[i])$.

7. A random number r was generated from a uniform distribution $U[0,1]$. This random number and the cdf $F(b|a = a[i])$ gives $b[i]$.

The procedure can be extended if there are more parameters.

6.6.3 Quasi-Monte Carlo Sample

A quasi-Monte Carlo sample can be obtained by using a pseudo-random number generator to select points from the admissible parameter space which is a closed

bounded interval in $\mathbb{R}$. A uniform p.d.f. and a p.d.f. generated from using a benchmark data set can be calculated as described above.

Chapter 7

Uncertainty Analysis

Under the assumption that the model form of tangential velocity v is known, radial velocity u and vertical velocity w can be predicted using equations from the Navier-Stokes system of equations. The question arises as to uncertainty in these predicted values resulting from uncertainty in the parameters of the models. To determine this uncertainty, a sample is generated from the set of admissible parameters that is associated with either a uniform distribution or a distribution containing information from benchmark data. Tangential wind v, radial wind u and vertical wind w are then calculated from this sample of parameters. The probability distributions over the parameter space is then assigned to each u, v and w. This defined probability distribution functions for u, v and w. The resulting statistics are used to evaluate uncertainty in the calculated wind values. The cumulative probability functions are used to find 90 % confidence regions for each wind component. The benchmark data for u, v and w are used for prediction validation of the models. The question arises concerning the accuracy of the predicted values of radial velocity u and vertical velocity w.

7.1 Information Theory

The state of information over the parameter space is central to the solution of the forward problem of prediction and the inverse problem of parameter resolution. Let S be a physical system consisting of an atmospheric vortex

and data measurements of the vortex. Let P be the finite N_p-dimensional parameter space that models S. In our case P is closed and bounded, therefore compact. Using the Lebesgue measurable subsets of P, a Lebesgue integrable function can be defined on the measurable subsets of P to define a uniform probability density function (p.d.f), $\mu(x) \equiv$ constant. This is the p.d.f. of null information representing the state of total ignorance on P. The content of information of any p.d.f. $f(x)$ is defined by Shannon [24]:

$$I(f, \mu) = \int f(x) \log\left(\frac{f(x)}{\mu(x)}\right) dx,$$

where log denotes the natural logarithm.

x is either a random variable or a random vector. This is also referred to as Kullback-Leibler divergence between two probability distributions, f and μ. This definition has the following properties (Tarantola 1982 [27]):

1. I is invariant with respect to a change of variables: $I(f, \mu) = I(f', \mu')$.
2. $I(f, \mu) \geq 0$
3. The information of the state of total ignorance is null: $I(\mu, \mu) = 0$. The reciprocal is also true: $I(f, \mu) = 0 \Rightarrow f = \mu$

$I(f, g)$ can be used to measure the distance between two distributions f and g, although it is not a metric because it is not symmetric and does not satisfy the triangle inequality.

The mutual information $M(x, y)$ between two random variables x and y with joint density $f(x, y)$ is defined as

$$M(x,y) = \int f(x,y) \log\left(\frac{f(x,y)}{f(x)f(y)}\right) dxdy,$$

where log denotes the natural logarithm.

Mutual information is a measure of the amount of information one random variable contains about another. Thus, the mutual information is the reduction in uncertainty of random variable x due to the knowledge of random variable y. Mutual information is symmetric so x says as much about y as y says about x. Let D denote the finite N_d-dimensional space of data. We can assume that the data is error free, or at least the uncertainties are small compared to the uncertainties in the parameters. Another reasonable assumption is that the data contains errors distributed according to a known p.d.f. The a posteriori probability distribution of the sample space S is defined in the present case to be $f(\mathbf{p},\mathbf{d}) = \mathbf{f}(\mathbf{d}|\mathbf{p})\mu(\mathbf{p})$, where $\mathbf{p}$ is the vector of parameters from a tangential wind model and $\mathbf{d}$ is the vector of data. In the case of identically distributed normal random errors with mean zero and variance σ^2 given by

$$\epsilon = \sum_{i=1}^{N_d} \left(d_i - v_i(\mathbf{p})\right)^2 = ||\mathbf{d} - \mathbf{v}\left(\mathbf{p}\right)||_{\mathbf{L_2}}^{\mathbf{2}}$$

the a posteriori p.d.f. becomes

$$f(\mathbf{d}|\mathbf{p}) = \mathbf{c_1}\exp\left[-\frac{\mathbf{1}}{\mathbf{2}}\frac{||\mathbf{d} - \mathbf{v}\left(\mathbf{p}\right)||^{\mathbf{2}}}{\sigma^{\mathbf{2}}}\right]$$

If $\mu(\mathbf{p})$ is the p.d.f. of null information, then

$$f(\mathbf{p},\mathbf{d}) = \mathbf{c_2}\exp\left[-\frac{\mathbf{1}}{\mathbf{2}}\frac{||\mathbf{d} - \mathbf{v}\left(\mathbf{p}\right)||^{\mathbf{2}}}{\sigma^{\mathbf{2}}}\right]$$

The uniform probability density function $\mu(x) \equiv$ constant exists as a p.d.f. and

$$f(\mathbf{p}, \mathbf{d}) = \mathbf{c_2} \exp\left[-\frac{\mathbf{1}}{\mathbf{2}} \frac{||\mathbf{d} - \mathbf{v}(\mathbf{p})||^{\mathbf{2}}}{\sigma^{\mathbf{2}}}\right]$$

exists uniquely as a p.d.f. under the assumptions:

1. The residuals $\epsilon_i = d_i - v_i(\mathbf{p})$, $i = 1, \cdots N_d$ are normally distributed with mean zero and constant variance σ^2.

2. There are a finite number of data and a finite number of parameters.

Parameters resolution is understood and evaluated in terms of marginal p.d.f.s, measures of central tendency, parameter correlations and joint parameter p.d.f.s.

7.2 Sensitivity Analysis

Sensitivity analysis, Saltelli [22], is the study of how the variation in the output of a model can be apportioned to different sources of variation and of how the given model depends upon the information fed into it. Sensitivity Analysis is used to increase the confidence in the model and its predictions by providing an understanding of how the model responds to changes in the inputs. Therefore, Sensitivity Analysis studies the relationships between information flowing in and out of the model. In this paper, Sensitivity Analysis is used to study the stability of the estimated parameters of a model and insensitivity with respect to small deviations from the assumptions about the underlying distribution assumed for the parameters. The goal of Sensitivity Analysis in this context is to determine if the various tangential wind models are sufficient to the task of modeling tangential wind and predicting radial and vertical winds.

7.2.1 Local Sensitivity Analysis

Local Sensitivity Analysis concentrates on the local impact of the factors on the model and is usually carried out by computing partial derivatives of the output functions with respect to the input variables.

Parameters p in the Tangential Wind Model ϕ

Local sensitivities relate small changes in ϕ to small changes in the parameters and can be used to measure the non-linearity of ϕ as a function of the parameters. Local Sensitivity Analysis is usually carried out by computing partial derivatives of the output functions with respect to the input variables. Consider an approximate Taylor series expansion at each point r_j:

$$\phi(r_i, \mathbf{p} + \mathbf{\Delta p}) = \phi(r_i, \mathbf{p}) + \sum_{j=1}^{N_p} \frac{\partial \phi}{\partial p_j} \Delta p_j + \frac{1}{2} \sum_{k=1}^{N_p} \sum_{j=1}^{N_p} \frac{\partial^2 \phi}{\partial p_k \partial p_j} \Delta p_k \Delta p_j$$

The partial derivatives $\partial\phi/\partial p_j = D_{p_j}\phi(r_i, \mathbf{p})$ are called first-order local sensitivity coefficients. Each $\partial\phi/\partial p_j$ is a linear estimate of the number of units change in ϕ as a result of a unit change in the parameter p_j. The local sensitivity coefficients can be normalized so that they do not depend on any units:

$$S_j(r_i, \mathbf{p}) = p_j \frac{\partial \phi}{\partial p_j}(r_i, \mathbf{p})$$

The following coefficients are a measure of the non-linearity of ϕ as a function of the parameters:

$$D^2_{p_k p_j}\phi(r_i, \mathbf{p}) = p_k p_j \frac{\partial^2 \phi}{\partial p_k \partial p_j}(r_i, \mathbf{p})$$

There are some models for which it is not possible to uniquely estimate all of the parameters. Parameters can be uniquely estimated if the local sensitivity coefficients over the range of the observations are not linearly dependent, in other words, if

$$a_1 S_1(r_i, \mathbf{p}) + a_2 S_2(r_i, \mathbf{p}) + \cdots + a_p S_p(r_i, \mathbf{p}) = 0$$

for all $i = 1, 2, \cdots, N_d$ only when $a_1 = a_2 = \cdots = a_p = 0$. Derivation of this can be found in Beck, [3]. The graphs of S_j vs r can help to determine the linear dependence of the local sensitivity coefficients.

The sensitivity coefficients can be used to approximate the variance of any non-linear function ϕ by using the Taylor Series expansion and computing $Var(\phi) = \mathbf{c}^T V \mathbf{c}$ where $\mathbf{c}^T$ is the vector with entries $\partial\phi/\partial p_j = D_{p_j}\phi(r_i, \mathbf{p})$ and V is the covariance matrix of the parameters. In other words, if there are three parameters a, b and c, then

$$V = \begin{bmatrix} \sigma_a^2 & r_{ab}^2 & r_{ac}^2 \\ r_{ab}^2 & \sigma_b^2 & r_{bc}^2 \\ r_{ac}^2 & r_{bc}^2 & \sigma_c^2 \end{bmatrix}$$

The parameters are estimated by minimizing the objective or cost function:

$$J(\mathbf{p}) = \frac{1}{2} \sum_{i=1}^{N} \left(\phi(r_i, \mathbf{p}) - \phi_{obs}(r_i)\right)^2$$

The derivatives of the objective function are:

$$D_{p_k} J(\mathbf{p}) = \sum_{i=1}^{N} \left(\phi(r_i, \mathbf{p}) - \phi_{obs}(r_i)\right) D_{p_k}\phi(r_i, \mathbf{p})$$

$$D^2_{p_k p_j} J(\mathbf{p}) = \sum_{i=1}^{N} \left[D_{p_k}\phi(r_i, \mathbf{p}) D_{p_j}\phi(r_i, \mathbf{p}) + \left(\phi(r_i, \mathbf{p}) - \phi_{obs}(r_i)\right) D^2_{p_k p_j}\phi(r_i, \mathbf{p})\right]$$

for $k = 1, \cdots N_p$.

Minimization of the objective function $J(\mathbf{p})$ involves finding parameters $\hat{p}_k$ such that $D_{p_k} J(\hat{\mathbf{p}}) = 0$ for all $k = 1, \cdots N_p$. Let $F_k(\mathbf{p}) = D_{p_k} J(\hat{\mathbf{p}}) = 0$. The determinant, D, of the matrix with entries

$$D^2_{p_k p_j} J(\mathbf{p}) = \frac{\partial^2 J(\mathbf{p})}{\partial p_k \partial p_j}$$

can be used to determine the existence of a unique minimum for $J(\mathbf{p})$. If D is positive definite, there is a unique minimum, [3]. The matrix D is positive definite if all its eigenvalues are positive.

The Parameter ν

Parameter ν does not appear in the model equation for tangential velocity and therefore is assumed independent of the parameters in this model. This parameter is assumed to be uniformly distributed in a set determined from physical principles and is found in the equations used to predict radial and vertical velocities. Sensitivity to this parameter can be computed from equation. $U = \frac{\partial u}{\partial \nu}$. U satisfies the following system:

$$
\begin{aligned}
U'(t) &= \left[\frac{\phi_t}{\phi} - \left(\frac{1}{t} + \frac{\phi_t}{\phi}\right)\frac{\psi\psi_{zz}}{\psi_z^2}\right] U \\
&+ \left[\left(\frac{\phi_{tt}}{\phi} + \frac{\phi_t}{t\phi} - \frac{1}{t^2}\right)\left(\frac{\psi\psi_{zz}}{\psi_z^2} - 1\right) - \frac{\psi_{zzz}}{\psi_z} + \frac{\psi_{zz}^2}{\psi_z^2}\right] \\
U(t_0) &= U_0
\end{aligned} \tag{7.1}
$$

$U(t_0) = U_0$ can be approximated numerically by

$$U_0 \approx \frac{u(t_0, \nu_2) - u(t_0, \nu_1)}{\nu_2 - \nu_1}$$

The Euler method can now be used to solve (7.1) for U.

7.2.2 Variance-Based Sensitivity Analysis

Variance-Based Sensitivity Analysis is a global method that apportions the output uncertainty to the uncertainty in the input factors [22]. This is usually done by probability density functions defined on the admissible set of parameters, thus the technique incorporates the influence of the whole range of variation and the form of the p.d.f. of the input.

The nonlinear regression model was given as $Y_n = \phi(r_n, \mathbf{p}) + \epsilon_n$ where ϵ_n is the random variable representing the stochastic or disturbance part of the model with $E(\epsilon_n) = 0$ and $Var(\epsilon_n) = \sigma^2$. For analysis purposes, [22], a collection of models of the form $y = E(Y|\mathbf{x}) + \epsilon$ is considered to describe the non-linear regression model in probabilistic terms. Here $\mathbf{x}$ contains some subset of $\mathbf{p}$. The total variation of the model prediction Y is defined as

$$Var[Y] = \int_{\Omega_Y} \left(y - E(y)\right)^2 p_Y(y)\ \mathrm{dy}$$

where Ω_Y is the domain of definition of Y, $E(Y)$ is the expected value or mean of Y and $p_Y(y)$ is the p.d.f. of Y. For example, Y can be the tangential wind considered as a random variable at a distance from the vortex center. This random variable Y is assumed to depend on the parameters $\mathbf{p}$ in the model which are also considered as random variables over the space of admissible parameters. Let $\mathbf{x}$ contain some subset of $\mathbf{p}$. Let $p_X(x)$ be the marginal p.d.f. of $\mathbf{x}$ and let $p_{Y|X}(y)$ be the conditional p.d.f. of y conditioned on knowledge of $\mathbf{x}$. Let Ω_X be the space of admissible parameters of subset $\mathbf{x}$ of $\mathbf{p}$ and note that

$$p_Y(y) = \int_{\Omega_X} p_{Y|X} p_X(x) \text{ dx}$$

Apportion the variance $Var[Y]$ as follows:

$$\begin{aligned}
Var[Y] &= \int_{\Omega_Y} (y - E(y))^2 p_Y(y) \text{ dy} \\
&= \int_{\Omega_Y} (y - E(y))^2 \int_{\Omega_X} p_{Y|X}(y) p_X(x) \text{ dx dy} \\
&= \int_{\Omega_Y} \int_{\Omega_X} (y - E(y))^2 p_{Y|X}(y) p_X(x) \text{ dx dy} \\
&= \int_{\Omega_Y} \int_{\Omega_X} (y - E(Y|X) + E(Y|X) - E(y))^2 p_{Y|X}(y) p_X(x) \text{ dx dy}
\end{aligned}$$

This simplifies to:

$$= \int_{\Omega_Y} \int_{\Omega_X} (y - E(Y|X))^2 p_{Y|X}(y) p_X(x) \text{ dx dy} \tag{7.2}$$

$$+ 2 \int_{\Omega_Y} \int_{\Omega_X} (y - E(Y|X)) (E(Y|X) - E(y)) p_{Y|X}(y) p_X(x) \text{ dx dy} \tag{7.3}$$

$$+ \int_{\Omega_Y} \int_{\Omega_X} (E(Y|X) - E(y))^2 p_{Y|X}(y) p_X(x) \text{ dx dy} \tag{7.4}$$

Looking at each term separately starting with (7.2):

$$\int_{\Omega_Y}\int_{\Omega_X}\left(y-E(Y|X)\right)^2 p_{Y|X}(y)p_X(x)\ \mathrm{dx}\ \mathrm{dy}$$
$$=\int_{\Omega_X} Var(Y|X)p_X(x)\ \mathrm{dx}=E_{\mathbf{x}}(Var[Y|\mathbf{x}])$$

This term measures the variation of Y that is independent of the parameters in $\mathbf{x}$. The second term, (7.3), can be seen to be zero as follows:

$$\int_{\Omega_Y}\int_{\Omega_X}\left(y-E(Y|X)\right)\left(E(Y|X)-E(y)\right)p_{Y|X}(y)p_X(x)\ \mathrm{dx}\ \mathrm{dy}$$
$$=\int_{\Omega_Y}\int_{\Omega_X}\left(yE(Y|X)\right)p_{Y|X}(y)p_X(x)\ \mathrm{dx}\ \mathrm{dy}$$
$$-\int_{\Omega_Y}\int_{\Omega_X}\left(yE(y)\right)p_{Y|X}(y)p_X(x)\ \mathrm{dx}\ \mathrm{dy}$$
$$-\int_{\Omega_Y}\int_{\Omega_X}\left(E(Y|X)\right)^2 p_{Y|X}(y)p_X(x)\ \mathrm{dx}\ \mathrm{dy}$$
$$+\int_{\Omega_Y}\int_{\Omega_X}\left(E(Y|X)E(y)\right)p_{Y|X}(y)p_X(x)\ \mathrm{dx}\ \mathrm{dy}$$
$$=\left(E(y)\right)^2-\left(E(y)\right)^2-\left(E(y)\right)^2+\left(E(y)\right)^2=0$$

The third term, (7.4), results in:

$$\int_{\Omega_Y}\int_{\Omega_X}\left(E(Y|X)-E(y)\right)^2 p_{Y|X}(y)p_X(x)\ \mathrm{dx}\ \mathrm{dy}$$
$$=\int_{\Omega_X}\left(E(Y|X)-E(y)\right)^2 p_X(x)\ \mathrm{dx}=Var_{\mathbf{x}}[E(Y|\mathbf{x})]$$

This term measures the variation in $Var(Y)$ that results from knowledge

of parameters in $\mathbf{x}$. If $E_{\mathbf{x}}(Var[Y|\mathbf{x}]) = 0$, then the parameters in $\mathbf{x}$ have no contribution to the variance of Y and therefore no influence in the model's accuracy or ability to predict other quantities. Therefore, the closer this value is to one, the more important $\mathbf{x}$ is as an influence on Y. In summary, the prediction variance of Y can be written as:

$$Var[Y] = Var_{\mathbf{x}}[E(Y|\mathbf{x})] + E_{\mathbf{x}}(Var[Y|\mathbf{x}])$$

In this expression, $Var_{\mathbf{x}}[E(Y|\mathbf{x})]$ is called the variance of the conditional expectation and is a measure of the importance of $\mathbf{x}$ as it relates to Y. The second term, $E_{\mathbf{x}}(Var[Y|\mathbf{x}])$, is called the residual term. This term measures the remaining variability in y that is due to other unobserved inputs or other unknown sources of variation when $\mathbf{x}$ is fixed. The correlation ratio was defined by McKay [17] as:

$$\eta^2 = \frac{Var_{\mathbf{x}}[E(Y|\mathbf{x})]}{Var[Y]} \tag{7.5}$$

If there are outliers in the data, the following modification is recommended:

$$\eta^2 = \frac{Var_{\mathbf{x}}\log\,[E(Y|\mathbf{x})]}{Var[\log\,Y]}$$

Chapter 8

Estimation and Analysis of the Wood-White Vortex 2 Tangential Wind Model

The normalized Wood-White Vortex 2 tangential wind model is of the form:

$$\phi(r) = \frac{\eta r^b}{a + br^\eta}$$

where $\eta = a + b, a > 0, b > 0$

and r is the distance from the vortex center.

The term r^b in the numerator models one- and two-cell vortices by controlling the behavior of the inner core. The denominator controls the decay of the vortex as $r \to \infty$. This tangential vortex model is normalized so that $\phi(r)$ is equal to one when r is equal to one and is dependent on parameters a and b. This dependence will be recognized by adding the vector $\mathbf{p}^T = (a\ b)$ to the list of independent variables of ϕ. In this manner, we write $\phi(r, \mathbf{p})$ as the expectation function in the non-linear model. An expectation function is non-linear if at least one of the derivatives of the expectation function with respect to the parameters depends on at least one of the parameters. For the Wood-White vortex 2 tangential wind model, both $\frac{\partial \phi}{\partial a}$ and $\frac{\partial \phi}{\partial b}$ depend on both parameters a and b and therefore is a non-linear model.

8.1 Parameters of ϕ

The Wood-White vortex 2 model was fitted to the Davies-Jones profile at the $z = 1$, 2, and 3 vertical levels representing 42 m, 84 m, and 126 m, respectively., above the surface using $0.0001 \leq a \leq 4.0001$ and $0.0001 \leq b \leq 4.0001$. The optimal parameter values of $\hat{p}_1 = \hat{a}$ and $\hat{p}_2 = \hat{b}$ were calculated by minimizing the objective function

$$J(\mathbf{p}) = \sum_{i=1}^{N} \left(\phi(r_i, \mathbf{p}) - \phi_{obs}(r_i)\right)^2 = \sum_{i=1}^{N} \left(\phi(r_i, \mathbf{p}) - z_i\right)^2$$

using grid spacing of 0.01 for each of the parameters. The optimal parameter values at the levels $z = 1$, 2, and 3 were calculated and listed in Table 8.1.

Table 8.1: Optimal Parameters

height z	$\hat{a}$	$\hat{b}$	$J(\hat{\mathbf{p}})$	$\hat{\sigma}^2$
1	1.7701	1.0501	0.0018	0.000065
2	1.8201	1.0301	0.0021	0.000075
3	1.8801	1.0101	0.0027	0.000096

Essentially the same values were obtained using Steepest Descent. Joint probability density functions (p.d.f.s) were estimated for the parameters using the function $f(\mathbf{p}) = \exp(-J(\mathbf{p}))$, normalized so that the volume under the surface was equal to one. An example joint p.d.f. over the intervals $0.1 \leq a \leq 4.01$ and $0.1 \leq b \leq 4.01$ is illustrated in Figure 8.1.

From the joint p.d.f.s, marginal p.d.f.s for the parameters a and b were estimated at various grid points. Using the joint p.d.f. for parameters a and b in Wood-White vortex 2 model, marginal p.d.f.s were calculated at levels $z = 1$, 2, and 3. Figure 8.2 shows the marginal distributions for a and b at level $z = 1$. The marginal distributions at levels $z = 2$ and $z = 3$ were virtually identical in form.

Figure 8.1: Example joint pdfs for a and b

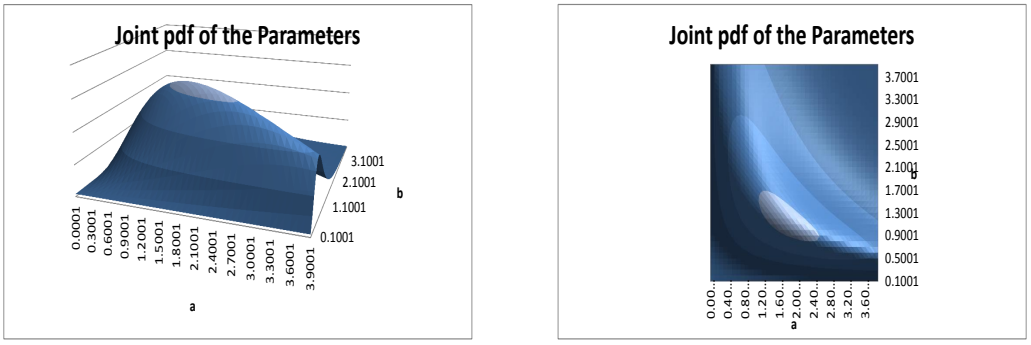

Figure 8.2: Marginal pdfs for a and b

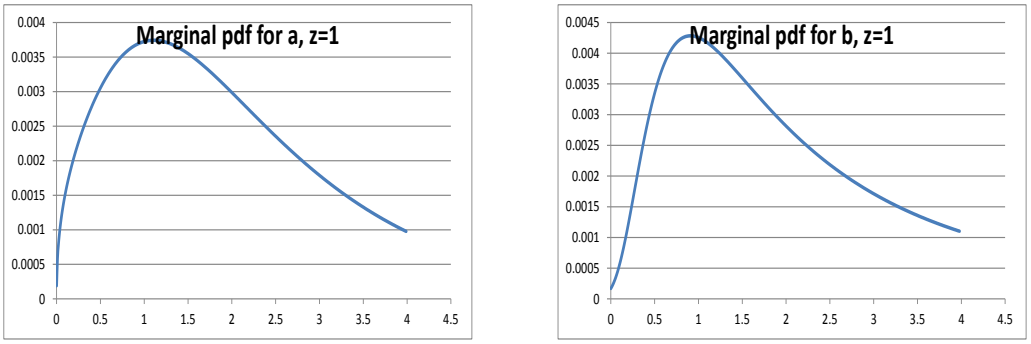

Using the marginal p.d.f.s for the parameters, the mean and standard deviation of each parameter, a and b, were calculated at levels z =1, 2, and 3 and are summarized in Table 8.2. The means for b are larger than the estimates for b because the marginal p.d.f.s are highly skewed, however, the estimate is within one standard deviation of the mean at each level.

Table 8.2: Statistics for the Parameters

height z	$\hat{a}$	μ_a	σ_a	$\hat{b}$	μ_b	σ_b
1	1.7701	1.7229	0.9955	1.0501	1.7186	0.9807
2	1.8201	1.7371	0.9972	1.0301	1.7155	0.9792
3	1.8801	1.7590	0.1000	1.0100	1.7100	0.9770

Information content, $I(a)$ and $I(b)$, of each parameter and mutual information, $I(a, b)$, contained in parameters a and b were calculated and are given

in Table 8.3. The information content is a measure of the information in the Davies-Jones tangential wind data that is contained in the parameters a and b. Information content is relative, so the actual number is not as important as the ratio of the two numbers. With this in mind, parameter b contains more information from the data than parameter a over the entire tangential wind profile, but both are of the same magnitude of importance. This corroborates conclusions from the marginal p.d.f.s of the parameters. Recall that parameter b controls the shape of the inner core of the vortex. The marginal p.d.f. for b is more defined than the marginal p.d.f. for a and has a smaller standard deviation, however, both standard deviations are large. The parameters have a large mutual information content compared to their individual information contents which implies that they are not independent. This will be seen later in their correlation coefficient. The parameters a and b are correlated as an artifact of non-linear least squares estimation. It is also interesting to notice that the information content does not vary significantly between levels.

Table 8.3: Information Content of Parameters

height z	$I(a)$	$I(b)$	$I(a,b)$
1	0.072	0.105	0.117
2	0.069	0.106	0.116
3	0.065	0.109	0.114

Variance-based sensitivity was calculated for each parameter at every available distance r from the vortex center. Some representative values are given in Table 8.4 at level $z = 1$. The pattern indicates the importance of parameter a at the end of the profile, and the importance of parameter b near the vortex center. This makes sense because parameter a controls the decay of the vortex as $r \to \infty$ and parameter b controls the shape of the inner core near the vortex

center. The R given in Table 8.4 is the correlation ratio for the parameter. There were no outliers, therefore equation 7.5 was used to calculate the correlation ratio. Correlation ratios are ratios of the variance of the estimate of tangential wind given knowledge of the parameter to the total variance. The importance of parameter b is evident throughout the profile. The importance of parameter a grows and becomes more important than b at the end of the profile.

Table 8.4: Variance-based Sensitivity for the Parameters

distance r	R_a	R_b	$1 - R_a - R_b$
0.154	0.0777	0.8954	0.0269
0.385	0.0877	0.7180	0.1943
0.538	0.1135	0.5714	0.3152
0.769	0.1684	0.3634	0.4682
1.077	0.2871	0.1881	0.5249
1.3077	0.4102	0.1193	0.4704
1.5384	0.5300	0.0784	0.3917
1.8462	0.6555	0.0509	0.2936
2.0000	0.7027	0.0446	0.2527

The work in this section used a grid with spacing 0.01 over the parameters a and b. Since this provides 400 values for a and 400 values for b, the entire rectangular space consists of 160,000 pairs of parameter values. Three parameters in the tangential wind model Wood-White vortex 3 would involve thirty two million parameters combinations. Future models with four or more parameters could be computationally prohibitive for any real-time system, therefore, the use ot random samples is explored in calculating data on tangential, radial and vertical wind. For this purpose, random samples were generated and are described next. A pseudo-random sample S_1 of 10,000 pairs of parameters was generated using a uniform distribution for each parameter. The statistics are

given under the assumption of a uniform distribution and under the assumption of a distribution defined from the Davies-Jones data. The statistics for these samples are given below, where μ_a, σ_a^2, μ_b, σ_b^2 and r_{ab}^2 are the mean and variance of a, the mean and variance of b, and the correlation between a and b. The first table, Table 8.5, gives the statistics from a uniform distribution over a grid compared to a uniform distribution from the pseudo-random sample.

Table 8.5: Uniform Distribution for the Parameters

Source	μ_a	σ_a	μ_b	σ_b	r_{ab}^2
Grid	2.0001	1.1547	2.0001	1.1547	0.0000
S_1	1.9913	1.1549	2.0066	1.1634	-0.0023

Table 8.6 gives the statistics for a distribution defined by the Davies-Jones data set over the grid compared to a distribution defined by the Davies-Jones data set from the pseudo-random sample for level $z = 1$.

Table 8.6: Distribution Defined by DJ Data, Level 1

Source	μ_a	σ_a	μ_b	σ_b	r_{ab}^2
Grid	1.7229	0.9955	1.7186	0.9807	-0.4420
S_1	1.7154	1.9980	1.7258	0.9911	-0.4446

Table 8.7 gives the statistics for a distribution defined by the Davies-Jones data set over the grid compared to a distribution defined by the Davies-Jones data set from the pseudo-random sample for level $z = 2$.

Table 8.7: Distribution Defined by DJ Data, Level 2

Source	μ_a	σ_a	μ_b	σ_b	r_{ab}^2
Grid	1.7371	0.9972	1.7155	0.9792	-0.4404
S_1	1.7297	1.9998	1.7225	0.9896	-0.4430

Table 8.8 gives the statistics for a distribution defined by the Davies-Jones data set over the grid compared to a distribution defined by the Davies-Jones

data set from the pseudo-random sample for level $z = 3$.

Table 8.8: Distribution Defined by DJ Data, Level 3

Source	μ_a	σ_a	μ_b	σ_b	r^2_{ab}
Grid	1.7590	0.9997	1.7101	0.9768	-0.4381
S_1	1.7518	1.0025	1.7169	0.9971	-0.4407

For analysis purposis, the following random samples were generated:

1. Sample S_2 was generated consisting of 1000 pairs of parameters using a uniform distribution for each parameter. This sample was generated for comparison to the above sample S_1 and comparison to samples S_3 and S_4 described below.

2. Sample S_3 was generated consisting of 1000 pairs of parameters using the marginal distributions for a and b under the assumption that a and b are uncorrelated.

3. Sample S_4 was generated consisting of 1000 pairs of parameters using the Gibbs sampling algorithm from a joint p.d.f. for a and b using a grid with spacing 0.01 with $0.001 \leq a \leq 4.001$ and $0.001 \leq b \leq 4.001$. A Gibbs sample captures the correlation between a and b.

The statistics for these random samples are given in Table 8.9.

Table 8.9: Statistics for Random Samples, level $z = 1$

Source	$\hat{a}$	μ_a	σ_a	$\hat{b}$	μ_b	σ_b	r^2_{ab}
S_2	1.7701	2.0498	1.1569	1.0501	1.9798	1.1451	-0.0676
S_3	1.7701	1.6979	1.0072	1.0501	1.7650	1.0147	-0.0273
S_4	1.7701	1.7534	1.0188	1.0501	1.6792	0.9930	-0.4728

In all samples, the optimal estimate is within one standard deviation of the mean and the correlations are consistent with the sampling technique.

8.2 Tangential Wind v Through the Model ϕ

Figure 8.3 shows the Wood-White vortex 2 tangential wind profile fitted to the Davies-Jones tangential wind profile using grid spacing of 0.01 and the normalized residuals. The residuals for v are defined to be $d(r_i) = v(r_i, \hat{\mathbf{p}}) - z_i$ for $i = 1, \cdots N_d$, where we will write v instead of ϕ in what follows. The residuals are plotted versus r.

Figure 8.3: Tangential Profile and Residual Plots

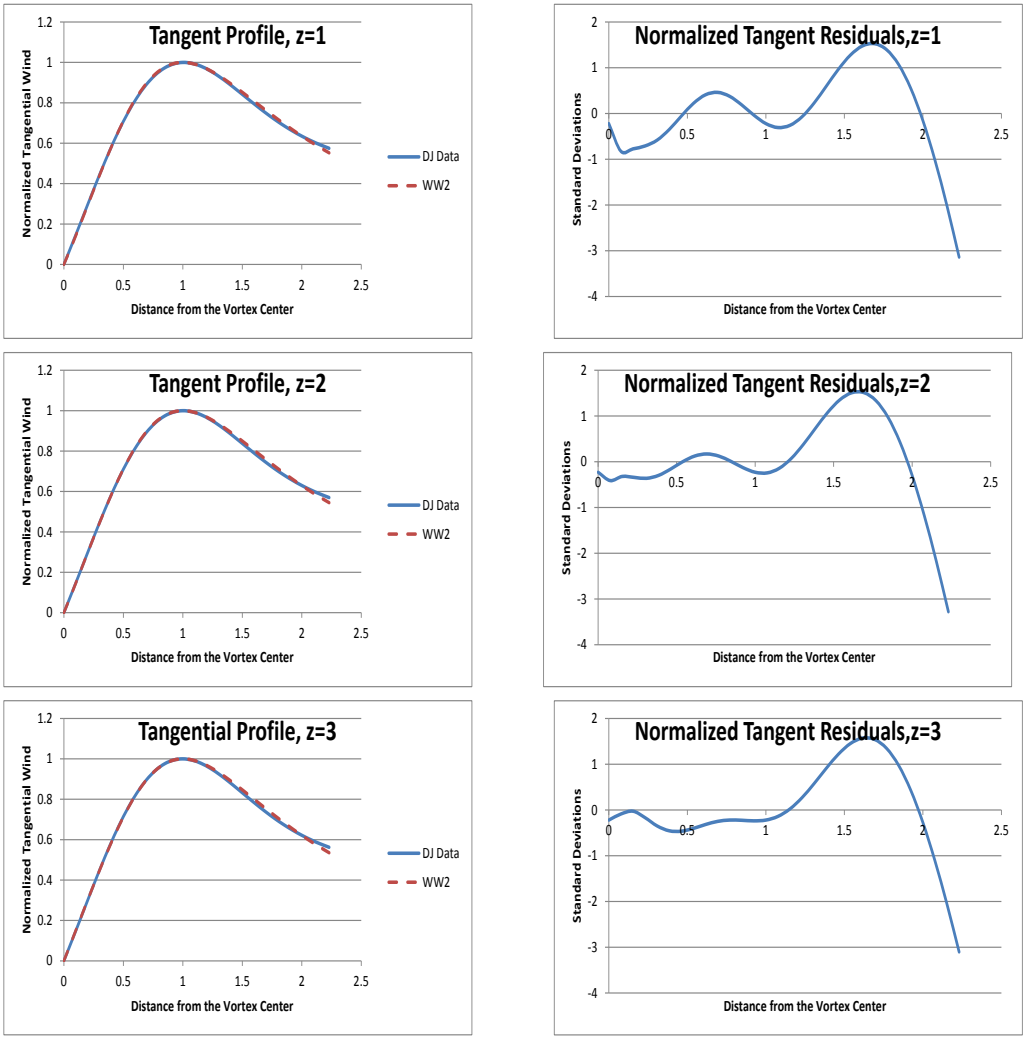

The mean, standard deviation, skewness and kurtosis of the residuals are

given in Table 8.10. The mean μ_R was within one standard deviation of zero. Hence, the mean of the residuals was not significantly different from zero. The plot of the residuals show that the distribution of the residuals was not uniform. The residuals at all three levels have coefficients of skewness that are negative which indicates that their distributions are all skewed to th left, The values of skewness and kurtosis will be used later in discussing normality of the distribution of the residuals.

Table 8.10: Statistics of the Residuals

height z	μ_R	σ_R	skew	Kurtosis
1	0.0017	0.0077	-0.0078	2.401
2	0.0019	0.0083	-0.0099	3.429
3	0.0021	0.0094	-0.0081	2.427

A runs test was used to test for randomness with results given in Table 8.11. In level $z = 1$, the expected number of runs was 13.857. The actual number was five which was almost four standard deviations below the mean,

Table 8.11: Runs Test Statistics

height z	V	N_1	N_2	μ_V	σ_V	test statistic
1	5	18	10	13.857	2.376	-3.727
2	5	18	10	13.857	2.376	-3.727
3	5	16	12	14.712	2.541	-3.823

The hypothesis of randomness is rejected. Therefore, the residuals are most likely correlated. The autocorrelation function was calculated and plotted versus lag. The bounds are plotted as dotted lines. The autocorrelation plots were similar at all levels, therefore only the plot for level $z = 1$ is given in Figure 8.4.

The plots of the residuals and the autocorrelation function both indicate large lags are needed for uncorrelated residuals. This shows a systematic cor-

Figure 8.4: Autocorrelation Function at Level $z = 1$

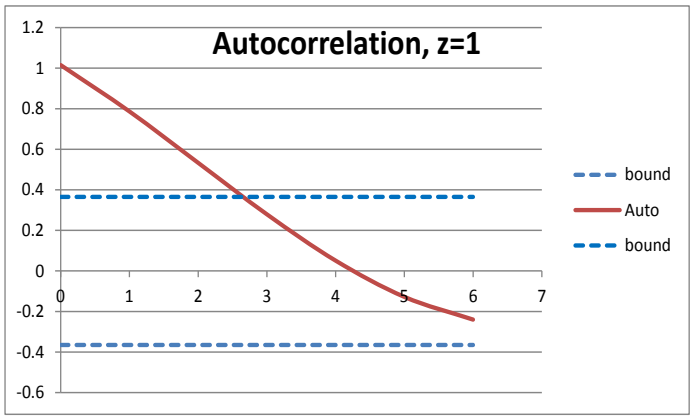

relation in the residuals. Next, the assumption of normality was tested at each of the different levels. Skewness s_k and kurtosis K are used in the Jarque-Bera test statistic JB. The Kolmogorov-Smirnov test for normality was conducted with test statistic D_N. All of these results are given in Table 8.12.

Table 8.12: Normality Test Statistics

height z	JB	D_N
1	7.206	0.111
2	14.701	0.211
3	7.363	0.209

Although the null hypothesis of normality could be rejected by the Jarque-Bera test, the critical value of the Kolmogorov-Smirnov test is 0.242 and therefore the null hypothesis of normality is not rejected under this test. The Jarque-Bera test statistic has a Chi-Square distribution with 2 degrees of freedom, and, for example, the critical value for the test is 5.991 for $\alpha = 0.05$. The Kolmogorov-Smirnov test is considered the better test for normality because it is less prone to rejection of the null hypothesis of normality when the hypothesis it true, therefore the null hypothesis of normality is not rejected here. Two plots were generated and are shown in Figure 8.5. The first plot contains the

cumulative distribution functions of the residuals and the cumulative distribution function of the normal distribution in order to observe the close agreement between the two distributions. The second plot contains the difference between these two distributions and was used to determine the Kolmogorov-Smirnov test statistic.

Figure 8.5: Residual and Normal cdfs, KS Test Statistic

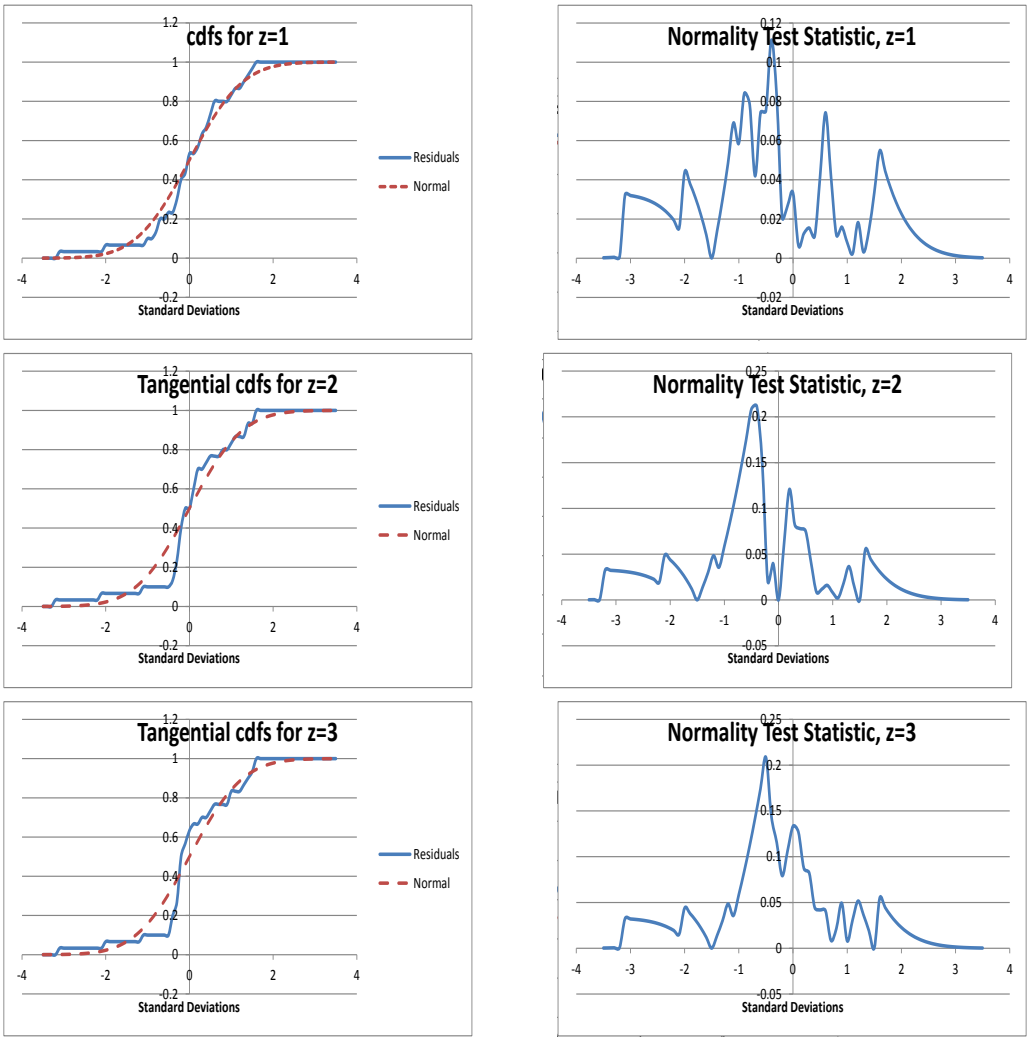

The pseudo-random samples described in the last section were used to generate a p.d.f. and a c.d.f. for tangential wind v and these were used to calculate statistics for v at levels $z = 1$, 2, and 3 for selected values of the distance from

the vortex center r. Shannon's information content of the p.d.f. for v was also calculated. This will be used later to compare information in v to information in predicted radial and vertical winds. The statistics for v at z = 1,2, and 3 are given in table 8.13 and table 8.14 for selected values of r. In the tables, $v(r)$ is the estimated value of v using the Wood-White vortex 2 model. Table 8.13 contains data using parameter pairs from the grid with spacing 0.01. Table 8.14 contains data using parameters pairs from the pseudo-random sample.

Table 8.13: Statistics for v, Grid Sample

height z	radius r	$v(r)$	μ_v	σ_v	$I(v)$
1	0.538	0.7537	0.6757	0.1684	0.2433
1	0.846	0.9756	0.9610	0.0241	0.2458
1	1.231	0.9593	0.9435	0.0352	0.2550
1	1.538	0.8351	0.8066	0.1115	0.2473
2	0.538	0.7545	0.6746	0.1685	0.2422
2	0.846	0.9755	0.9608	0.0242	0.2441
2	1.231	0.9588	0.9430	0.0354	0.2528
2	1.538	0.8324	0.8051	0.1120	0.2447
3	0.538	0.7548	0.6731	0.1688	0.2408
3	0.846	0.9753	0.9605	0.0244	0.2417
3	1.231	0.9580	0.9423	0.0357	0.2495
3	1.538	0.8288	0.8027	0.1126	0.2410

First, observe that the values in both tables are in close agreement, which indicates that the pseudo-random sample can be used to effectively calculate all data of interest. The means and standard deviations for v were used to create 80% error bars. Example plots are given in Figure 8.6. The first plot shows a comparison between the c.d.f.s for v with the uniform distribution and the distribution from the Davies-Jones data at a distance of r = 0.538 from the vortex center. This plot gives a visual demonstration of the value of the data in determining the value of v. It is related to the information in v which compares information content in distributions. In this case, the p.d.f. of v

Table 8.14: Statistics for v, Pseudo-Random Sample

height z	radius r	$v(r)$	μ_v	σ_v	$I(v)$
1	0.538	0.7537	0.6759	0.1688	0.2427
1	0.846	0.9756	0.9611	0.0242	0.2458
1	1.231	0.9593	0.9436	0.0352	0.2546
1	1.538	0.8351	0.8074	0.1113	0.2460
2	0.538	0.7545	0.6748	0.1690	0.2416
2	0.846	0.9755	0.9609	0.0243	0.2441
2	1.231	0.9588	0.9432	0.0354	0.2524
2	1.538	0.8324	0.8059	0.1118	0.2438
3	0.538	0.7548	0.6733	0.1692	0.2403
3	0.846	0.9753	0.9605	0.0245	0.2418
3	1.231	0.9580	0.9425	0.0357	0.2491
3	1.538	0.8288	0.8035	0.1124	0.2401

generated from the Davies-Jones data with the distribution generated from a uniform distribution over the parameter space via the pseudo-random sample. The slope of the graph at $v(r)$ is much larger for the c.d.f. with the Davies-Jones data than for the c.d.f. with uniformly distributed data, indicating more information. However the standard deviations are large in both which indicates a large amount of uncertainty in both distributions. This can be seen in the second plot which shows error bars around v using the two distributions over all the values of r where $0 \leq r \leq 2.231$.

The large error bars are a result of the large uncertainty in parameters a and b. Although incorporation of data reduces this uncertainty, the uncertainty is still large. The uncertainty can be reduced further with uncorrelated and Gibbs sampling. The data in table 8.15 is from level $z = 1$. Table 8.15 gives the actual value of v, the estimation of v from the sample and the standard deviation of v and shows the reduction of the standard deviation of v given a sample with more information. Table 8.15 also reveals the close agreement between data obtained from sample S_2 and data obtained from much larger

Figure 8.6: Tangential cdf and Error Bars

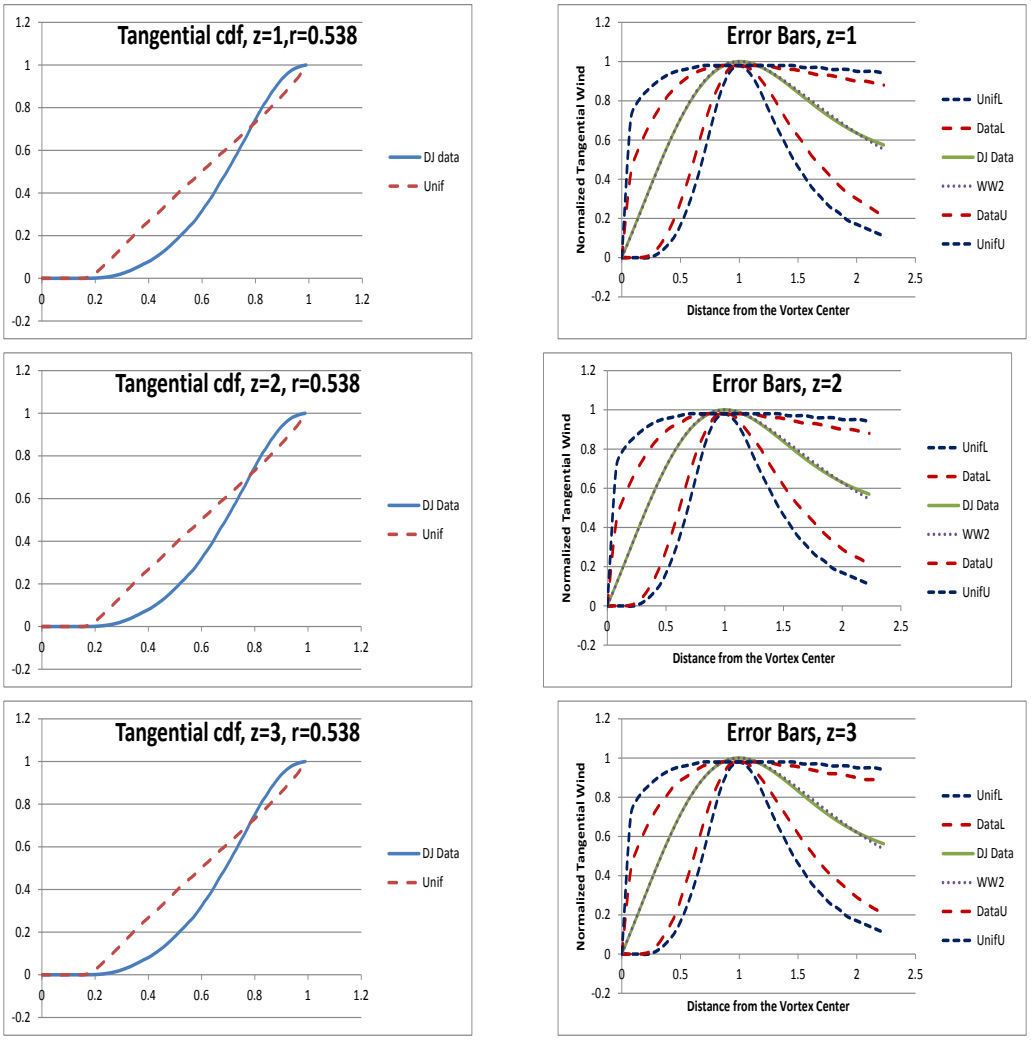

samples discussed earlier. This verifies the ability to predict the tangential wind v from small samples that could be obtained in real-time systems.

The Gibbs data set S_3 contains more information than the pseudo-random sample. Figure 8.7 shows the c.d.f.s generated from samples S_1 and S_3 at level $z = 1$ and the previous graph generated from the pseudo-random sample. This comparison illustrates the results of using a data set with more information.

Local sensitivity coefficients were calculated to examine the level of sensitivity of each parameter with respect to the distance from the vortex center

Table 8.15: Statistics for v from Small Samples

Sample	radius r	$v(r)$	μ_v	σ_v	$I(v)$
S_2	0.538	0.754	0.672	0.167	0.225
S_2	0.846	0.976	0.960	0.024	0.230
S_2	1.231	0.959	0.942	0.035	0.239
S_2	1.538	0.835	0.801	0.166	0.110
S_3	0.538	0.754	0.704	0.146	0.450
S_3	0.846	0.976	0.965	0.019	0.366
S_3	1.231	0.959	0.950	0.028	0.382
S_3	1.538	0.835	0.825	0.094	0.423
S_4	0.538	0.754	0.707	0.131	0.538
S_4	0.846	0.976	0.966	0.016	0.504
S_4	1.231	0.959	0.950	0.024	0.492
S_4	1.538	0.835	0.823	0.082	0.515

Figure 8.7: Pseudo-random sample and Gibbs c.d.f.s

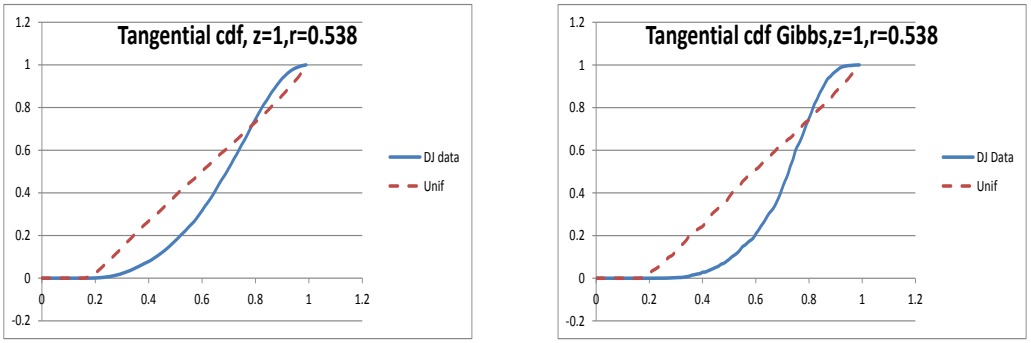

and also to determine linear independence of the local sensitivity coefficients. The graph of the local sensitivity coefficients shows linear independence and the greater sensitivity of v to the parameter b in the profile. The graph is given in Figure 8.8 for the level z=1 data:

The partial derivatives from the local sensitivity coefficients were used to calculate an approximate variance for v using the formula $Var(v) = \mathbf{c}^T V \mathbf{c}$ where $\mathbf{c}^T$ is the vector with entries $\partial v/\partial p_i$ and V is the covariance matrix of the parameters. Specifically,

Figure 8.8: Local Sensitivity Coefficients

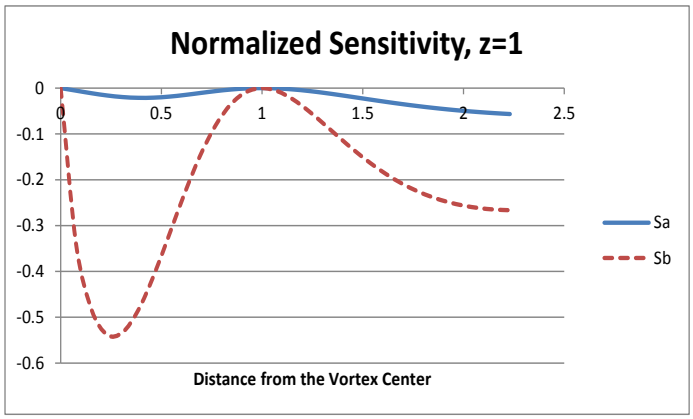

$$\mathbf{c}^T = \begin{pmatrix} \frac{\partial v}{\partial a} & \frac{\partial v}{\partial b} \end{pmatrix}$$

$$V = \begin{bmatrix} \sigma_a^2 & r_{ab}^2 \\ r_{ab}^2 & \sigma_b^2 \end{bmatrix}$$

Error bars were generated for v using the actual standard deviation of v, some of which are given in Table 8.12, and the approximate standard deviation computed as

$$\sigma_v = \sqrt{\mathbf{c}^T V \mathbf{c}}$$

The graph indicates that the approximate error bars can be used without much loss of information. The graph is given in Figure 8.9 for level z=1.

Lastly, the determinant, D, of the matrix with entries

$$D^2_{p_k p_j} J(\mathbf{p}) = \frac{\partial^2 J(\mathbf{p})}{\partial p_k \partial p_j}$$

was calculated and the eigenvalues for the matrix were determined. For level $z = 1$, the eigenvalues were $\lambda_1 = 3.574$ and $\lambda_2 = 0.884$ with matrix:

Figure 8.9: v with Approximate Error Bars

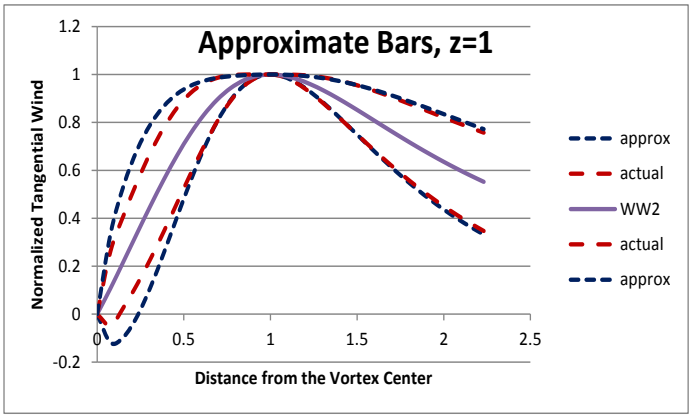

$$D^2J(\mathbf{p}) = \begin{bmatrix} 0.521 & 1.708 \\ 1.708 & 0.317 \end{bmatrix}$$

For level $z = 1$, the eigenvalues were $\lambda_1 = 3.718$ and $\lambda_2 = 0.838$ with matrix:

$$D^2J(\mathbf{p}) = \begin{bmatrix} 0.494 & 1.784 \\ 1.784 & 0.320 \end{bmatrix}$$

For level $z = 1$, the eigenvalues were $\lambda_1 = 3.882$ and $\lambda_2 = 0.790$ with matrix:

$$D^2J(\mathbf{p}) = \begin{bmatrix} 0.466 & 1.870 \\ 1.870 & -0.422 \end{bmatrix}$$

In all cases, the eigenvalues are positive which implies that the objective function J has a unique minimum in all three levels.

The next two sections study the feasibility of estimating radial and vertical winds if the tangential wind profile is known. This is the forward problem of prediction.

8.3 Radial Wind u

In the following, the Wood-White 2 vortex model was used to estimate ϕ. Recall that the tangential wind profile is expressed as a product

$$v(r, z) = \phi(r)\psi(z)$$

where ϕ gives the radial profile of the tangential wind and ψ gives the vertical profile of the maximum tangential wind. In the cylindrical case, $\psi \equiv 1$. In the non-cylindrical case, the model for the function ψ is

$$\psi(z) = V_x \tanh\left(\frac{A_1 z}{H}\right) \tanh\left(A_2\left(1 - \frac{z}{H}\right)\right)$$

where V_x is a parameter representing the maximum tangential velocity at the vertical level z. A_1, A_2 and H are parameters.

In the cylindrical case, the radial wind u was calculated using the tangential Navier-Stokes equation along with the conservation of mass equation given tangential wind v using equation (5.2). The radial velocity u is shown in figure 8.10.

Figure 8.10: Radial Wind Profile: Cylindrical Case

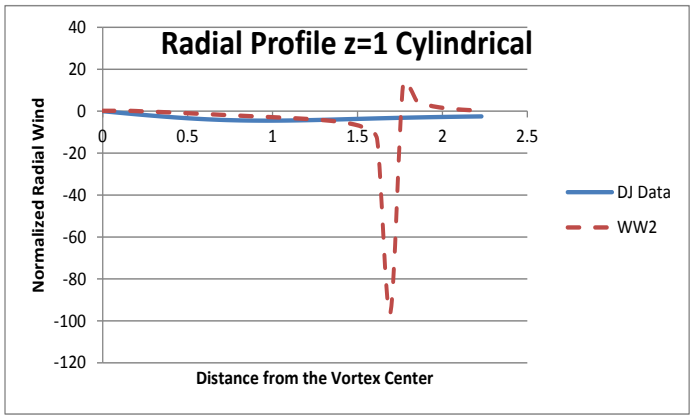

A singularity occurred at $r = 1.692$ and the profiles diverged over the entire region of interest. Although there are values of the parameters which result in no singularities in the u profile, these values are the exception rather than the rule. This is the primary reason for selecting the z-dependent profile for study. In the z-dependent profile case, the kinematic viscosity, ν, was first estimated from the data by least squares minimization of the error with the objective function

$$J = \sum_{i=1}^{N} \left(u(r_i, \nu) - u_{obs}(r_i)\right)^2$$

where $u(r_i, \nu)$ is the estimated radial wind calculated from equation (5.5) and $u_{obs}(r_i)$ is observation data from the Davies-Jones radial profile. Although different values were obtained for the different levels, a value of $\nu = 0.102$ worked well for all levels and was used in all the cases in this paper. The kinematic viscosity is a measure of the turbulent fluid flow divided by the laminar fluid flow. The turbulent flow is dominated by inertial forces, whereas the laminar flow is dominated by viscous forces. The method of characteristics was used to solve the ordinary differential equation (5.5) with initial data at the point of maximum tangential velocity r = 1.0. The tangential z-dependent wind profile must be assumed to solve equation (5.5). This profile and the parameters selected for this profile are described in section (6.1). The plots in figure 8.11 show the estimated radial wind profile $u(r)$ compared to the Davies-Jones radial wind profile $u_{obs}(r)$. The residuals $d(r_i) = u(r_i) - u_{obs}(r_i)$ for $i = 1, \cdots N_d$ were plotted versus r.

The mean, standard deviation, skewness and kurtosis of the residuals were computed. The mean μ_R was within one standard deviation of zero. Therefore, the mean of the residuals was not significantly different from zero. The plot of

Figure 8.11: Radial Wind Profile and Residuals

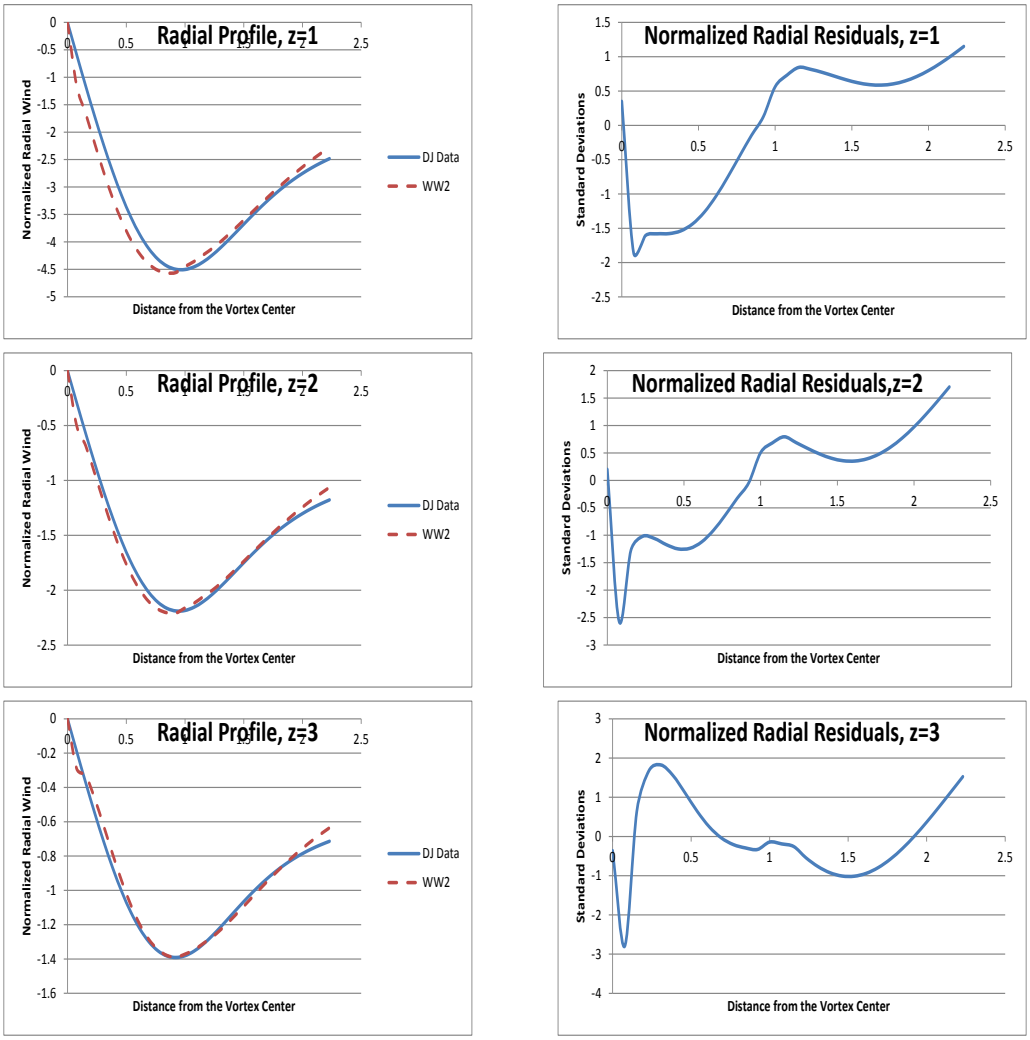

the residuals show that the distribution of the residuals was not uniform. The statistics of the residuals are given in Table 8.16.

A runs test was used to test for randomness with test statistic $T = -5.1$. The hypothesis of randomness is rejected. Therefore, the residuals are most likely correlated. Next, the assumption of normality was tested at each of the different levels. Skewness s_k and kurtosis K were used in the Jarque-Bera test statistic JB. The Kolmogorov-Smirnov test for normality was conducted with test statistic D_N. All of these results are given in Table 8.17.

Table 8.16: Statistics of the Residuals

height z	μ_R	σ_R	skew	Kurtosis
1	-0.0897	0.2562	-0.1901	-1.1342
2	-0.0153	0.0758	-0.0440	-0.1540
3	0.01500	0.0417	-0.0078	0.90370

Table 8.17: Normality Test Statistics

height z	JB	D_N
1	1.789	0.258
2	0.039	0.185
3	1.021	0.106

The null hypothesis of normality is rejected for the level $z = 1$ residuals by the Kolmogorov-Smirnov test for normality, therefore no conclusions can be made about these residuals in a least-squares statistical sense. It is interesting to note that the level $z = 1$ residuals do pass the Jarque-Bera test for normality. The remaining two levels pass both tests. The means and standard deviations of the radial residuals are larger than the residuals obtained for the tangential wind. This results in a loss of information.

Two plots were generated and are shown in figure 8.12. The first plot contains the cumulative distribution functions of the residuals and the cumulative distribution function of the normal distribution in order to observe the close agreement between the two distributions. The second plot contains the difference between these two distributions and was used to determine the Kolmogorov-Smirnov test statistic.

The pseudo-random samples were used to generate a p.d.f. and a c.d.f. for u and these were used to calculate statistics for u at levels $z = 1$, 2, and 3 for selected values of the distance from the vortex center r. Shannon's information content of the p.d.f. for u was also calculated. The statistics for u at $z = 1$,2,

Figure 8.12: Residual and Normal cdfs, KS Test Statistic

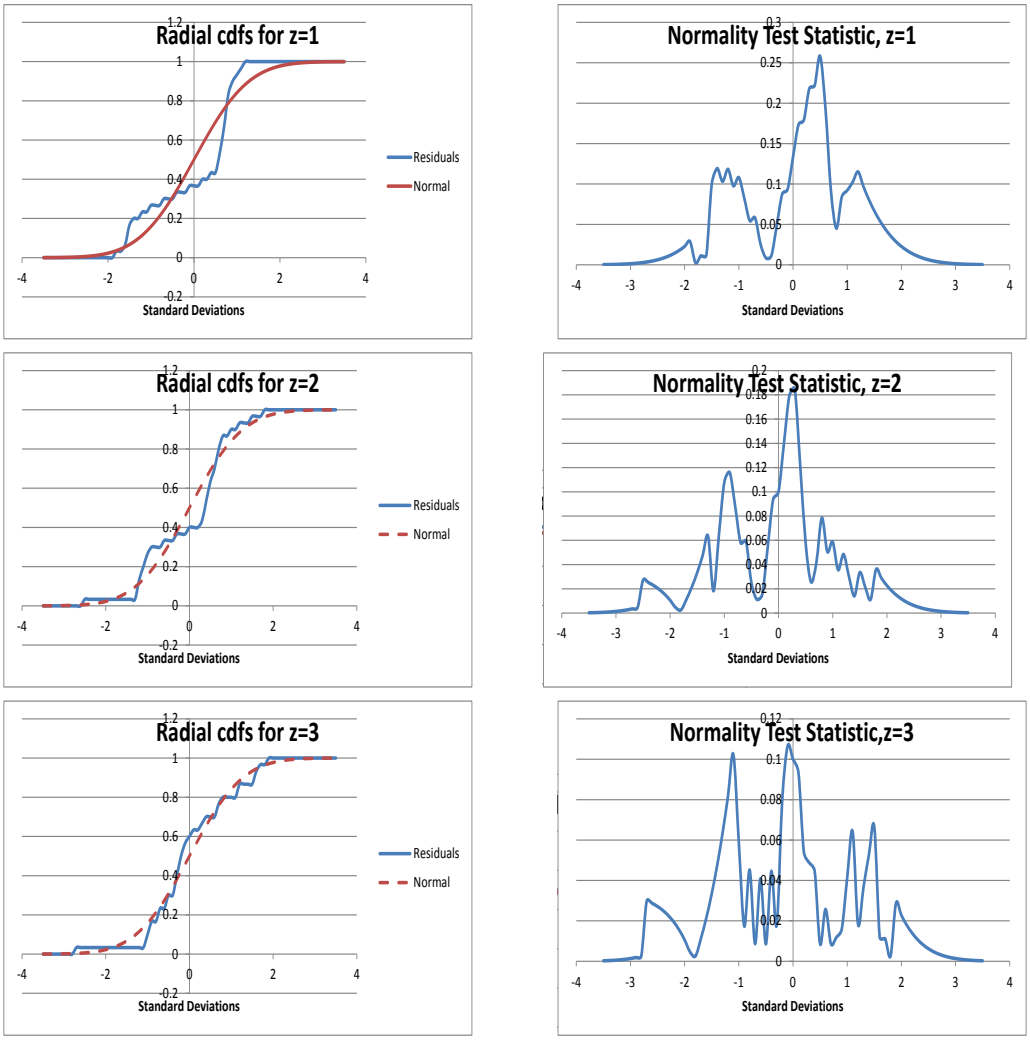

and 3 are given in table 8.18 and table 8.19 for selected values of r. In the tables, $u(r)$ is the estimated value of u using the Wood-White vortex 2 model. Table 8.18 contains data using parameter pairs from the grid with spacing 0.01. Table 8.19 contains data using parameters pairs from the pseudo-random sample.

The means and standard deviations for u were used to create 80% error bars. Example plots are given in figure 8.13. The first plot shows a comparison between the c.d.f.s for u with the uniform distribution and the distribution from

Table 8.18: Statistics for u, Grid Sample

height z	radius r	$u(r)$	μ_u	σ_u	$I(u)$
1	0.538	-3.9589	-3.7849	0.5009	0.2506
1	0.846	-4.5653	-4.6423	0.0738	0.2252
1	1.231	-4.1222	-4.0816	0.3259	0.2546
1	1.538	-3.5241	-3.4553	0.6511	0.2434
2	0.538	-1.8506	-1.7903	0.2477	0.2439
2	0.846	-2.2049	-2.2702	0.0666	0.1692
2	1.231	-2.0011	-2.0009	0.1960	0.2426
2	1.538	-1.6955	-1.6923	0.3668	0.2357
3	0.538	-1.0848	-1.0616	0.1585	0.1711
3	0.846	-1.3795	-1.4445	0.0616	0.2406
3	1.231	-1.2727	-1.2840	0.1631	0.2370
3	1.538	-1.0645	-1.0872	0.2883	0.2240

the Davies-Jones data at a distance of $r = 0.538$ from the vortex center. This plot demonstrates the value of the data in determining the value of u. The second plot shows error bars around u using the two distributions over all the values of r where $0 \leq r \leq 2.231$.

The large error bars are a result of the large uncertainty in tangential wind v. This uncertainty can be reduced further with uncorrelated and Gibbs sampling. The data in table 8.20 is from level $z = 1$. Table 8.20 gives the actual value of u, the estimation of u from the sample and the standard deviation of u and shows the reduction of the standard deviation of u given a sample with more information. Table 8.20 also reveals the close agreement between data obtained from sample S_2 and data obtained from much larger samples discussed earlier. This verifies the ability to predict the tangential wind u from small samples that could possibly be obtained real-time as in the case of tangential wind v.

The Gibbs data set S_3 contains more information than the pseudo-random sample. Figure 8.14 shows the c.d.f.s generated from samples S_1 and S_3 at level $z = 1$ and the previous graph generated from the pseudo-random sample. This

Table 8.19: Statistics for u, Pseudo-Random Sample

height z	radius r	$u(r)$	μ_u	σ_u	$I(u)$
1	0.538	-3.9589	-3.7861	0.5033	0.2504
1	0.846	-4.5653	-4.6418	0.0741	0.2240
1	1.231	-4.1222	-4.0838	0.3252	0.2539
1	1.538	-3.5241	-3.4603	0.6505	0.2424
2	0.538	-1.8506	-1.7909	0.2452	0.2231
2	0.846	-2.2049	-2.2706	0.0665	0.1729
2	1.231	-2.0011	-2.0025	0.1954	0.2423
2	1.538	-1.6955	-1.6945	0.3668	0.2341
3	0.538	-1.0848	-1.0616	0.1669	0.1592
3	0.846	-1.3795	-1.4441	0.0624	0.0616
3	1.231	-1.2727	-1.2850	0.1629	0.2225
3	1.538	-1.0645	-1.0888	0.2880	0.2230

comparison illustrates the results of using a data set with more information.

The radial wind u depends on the parameters a and b through the tangential wind v. A new parameter, the kinematic viscosity ν, is introduced in the computation of u. The parameter ν is not used in the computation of tangential wind v. Uncertainty in u depends on uncertainty in v as well as uncertainty in ν, therefore sensitivity analysis is needed to determine the sensitivity of u with respect to ν. The normalized sensitivity coefficient is $\nu\frac{\partial u}{\partial \nu}$ which has no units. The derivative $\frac{\partial u}{\partial \nu}$ can be computed from equation (5.5) and this equation is given again:

$$u'(t) = f(t,u) = \left[\frac{\phi_t}{\phi} - \left(\frac{1}{t} + \frac{\phi_t}{\phi}\right)\frac{\psi\psi_{zz}}{\psi_z^2}\right] u$$
$$+ \nu\left[\left(\frac{\phi_{tt}}{\phi} + \frac{\phi_t}{t\phi} - \frac{1}{t^2}\right)\left(\frac{\psi\psi_{zz}}{\psi_z^2} - 1\right) - \frac{\psi_{zzz}}{\psi_z} + \frac{\psi_{zz}^2}{\psi_z^2}\right]$$

Differentiating this equation with respect to ν gives the differential equation:

Figure 8.13: Radial cdf and Error Bars

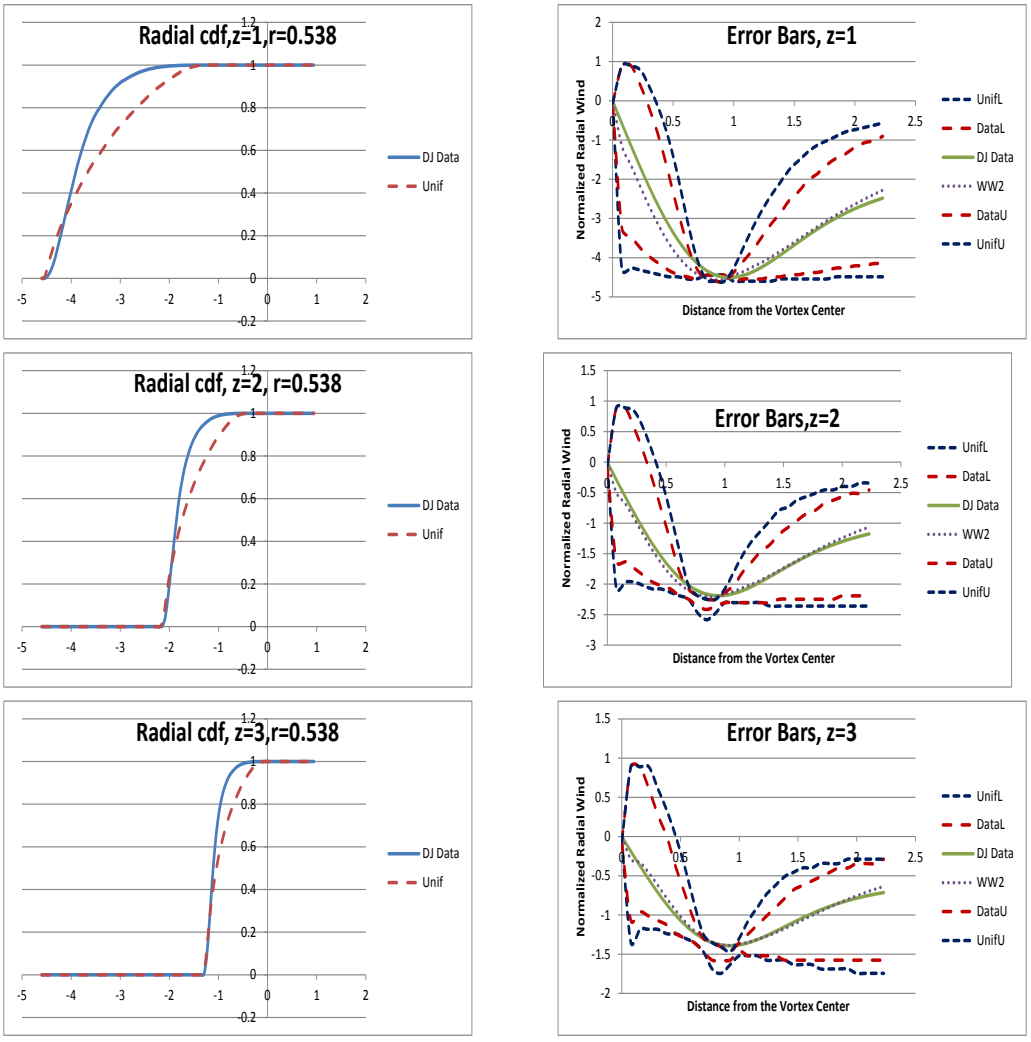

$$\frac{\partial}{\partial t}\left(\frac{\partial u}{\partial \nu}\right) = \left[\frac{\phi_t}{\phi} - \left(\frac{1}{t} + \frac{\phi_t}{\phi}\right)\frac{\psi\psi_{zz}}{\psi_z^2}\right]\left(\frac{\partial u}{\partial \nu}\right)$$
$$+ \nu\left[\left(\frac{\phi_{tt}}{\phi} + \frac{\phi_t}{t\phi} - \frac{1}{t^2}\right)\left(\frac{\psi\psi_{zz}}{\psi_z^2} - 1\right) - \frac{\psi_{zzz}}{\psi_z} + \frac{\psi_{zz}^2}{\psi_z^2}\right]$$
$$\frac{\partial u}{\partial \nu}(r_0) = du_0$$

This was solved using the Euler with the initial condition $\frac{\partial u}{\partial \nu}(r_0)$ estimated

Table 8.20: Statistics for u from Small Samples

Sample	radius r	$u(r)$	μ_u	σ_u	$I(u)$
S_2	0.538	-3.959	-3.777	0.494	0.231
S_2	0.846	-4.565	-4.644	0.073	0.209
S_2	1.231	-4.122	-4.069	0.319	0.236
S_2	1.538	-3.524	-3.421	0.642	0.226
S_3	0.538	-3.959	-3.874	0.413	0.397
S_3	0.846	-4.565	-4.631	0.059	0.335
S_3	1.231	-4.122	-4.137	0.267	0.371
S_3	1.538	-3.524	-3.561	0.560	0.385
S_4	0.538	-3.959	-3.895	0.357	0.512
S_4	0.846	-4.565	-4.624	0.050	0.411
S_4	1.231	-4,122	-4.139	0.227	0.500
S_4	1.538	-3.524	-3.544	0.492	0.487

Figure 8.14: Pseudo-random sample and Gibbs c.d.f.s

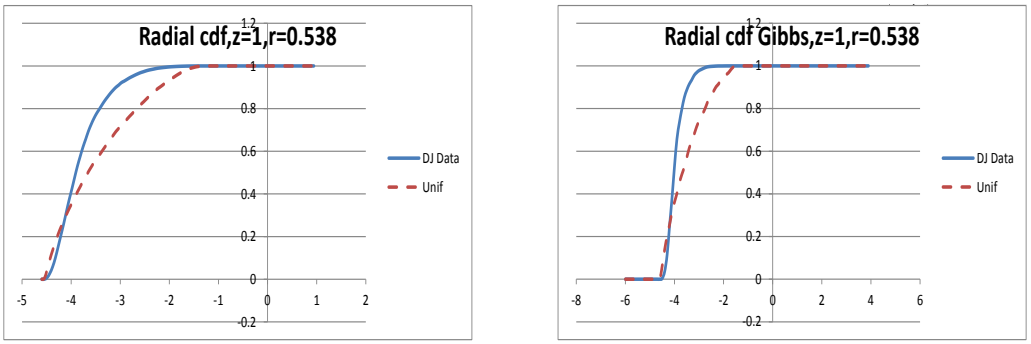

by a difference quotient of the radial profile at $r = 2$. The results are shown in figure 8.15 for level $z = 1$ and indicate that sensitivity with respect to ν is largest near the location of maximum tangential wind. It should be noted that the 80% error bars in the plots of figure 8.13 include the assumed error distribution of kinematic viscosity ν. For simplicity, ν was assumed to be uniformly distributed over the interval [0.051, 0.153].

Figure 8.15: Local Sensitivity with repect to ν

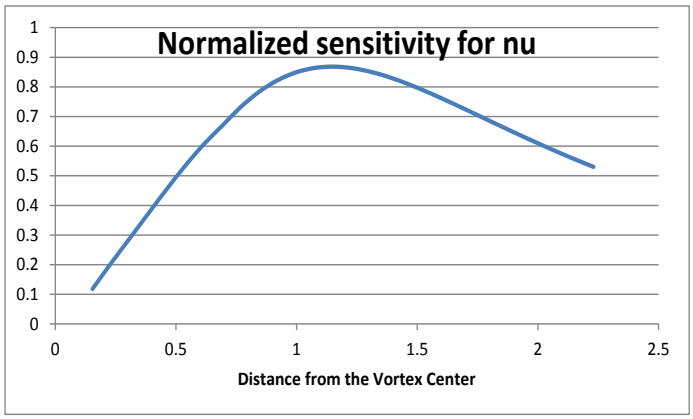

8.4 Vertical Wind w

In the following, the Wood-White 2 vortex model was used to estimate tangential profile v which was used to estimate radial profile u. The radial profile u was then used to estimate the vertical profile w.

For the cylindrical case, the vertical velocity w was calculated by equation (5.3) and the profile is shown in the figure 8.16.

Figure 8.16: Vertical Wind Profile: Cylindrical Case

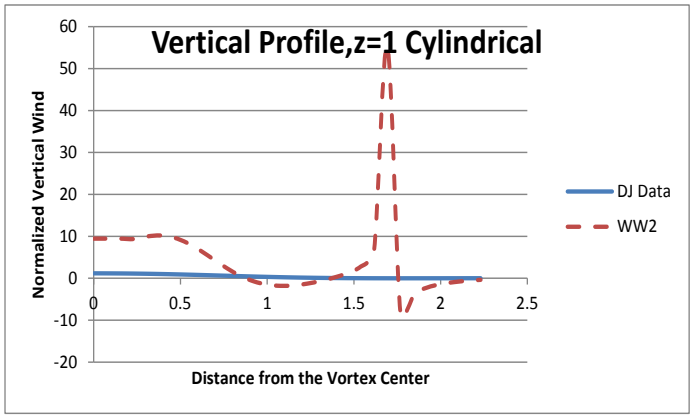

The singularity occurred at $r = 1.692$ in the radial and vertical profiles. The Wood-White vortex 2 and Davies-Jones data profiles diverged over the entire region of interest.

The vertical wind w was calculated using the tangential Navier-Stokes equation along with the conservation of mass equation (5.4). Figure 8.17 show Wood-White vortex 2 vertical wind profile compared to the Davies-Jones vertical wind profile. The residuals $d(r_i) = w(r_i) - w_{obs}(r_i)$ for $i = 1, \cdots N_d$ were plotted versus r. The vertical profiles did not differ in the three levels, so only level $z = 1$ is given in this section.

Figure 8.17: Vertical Wind Profile and Residuals

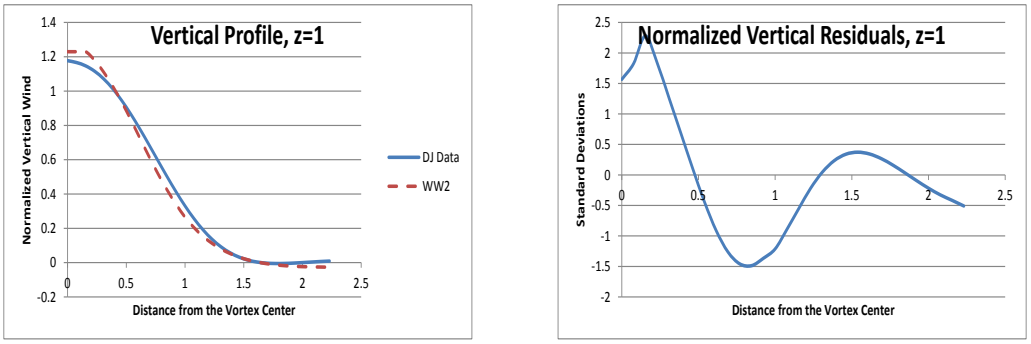

The mean, standard deviation, skewness and kurtosis of the residuals were computed. The mean μ_R was within one standard deviation of zero. Therefore, the mean of the residuals was not significantly different from zero. The plot of the residuals show that the distribution of the residuals was not uniform.

Table 8.21: Statistics of the Residuals

height z	μ_R	σ_R	skew	Kurtosis
1	-0.0143	0.0425	0.0243	-0.0514

A runs test was used to test for randomness with test statistic $T = -4.5802$. The hypothesis of randomness is rejected. Therefore, the residuals are most likely correlated. Next, the assumption of normality was tested at each of the different levels. Skewness s_k and kurtosis K were used in the Jarque-Bera test statistic JB. The Kolmogorov-Smirnov test for normality was conducted with

test statistic D_N. All of these results are given in the table below:

Table 8.22: Normality Test Statistics

height z	JB	D_N
1	0.0063	0.2581

The null hypothesis of normality if rejected by the Kolmogorov-Smirnov test, although accepted by the Jarque-Bera test. Two plots were generated and are shown in figure 8.18. The first plot contains the cumulative distribution functions of the residuals and the cumulative distribution function of the normal distribution in order to observe the close agreement between the two distributions. The second plot contains the difference between these two distributions and was used to determine the Kolmogorov-Smirnov test statistic.

Figure 8.18: Residual and Normal cdfs, KS Test Statistic

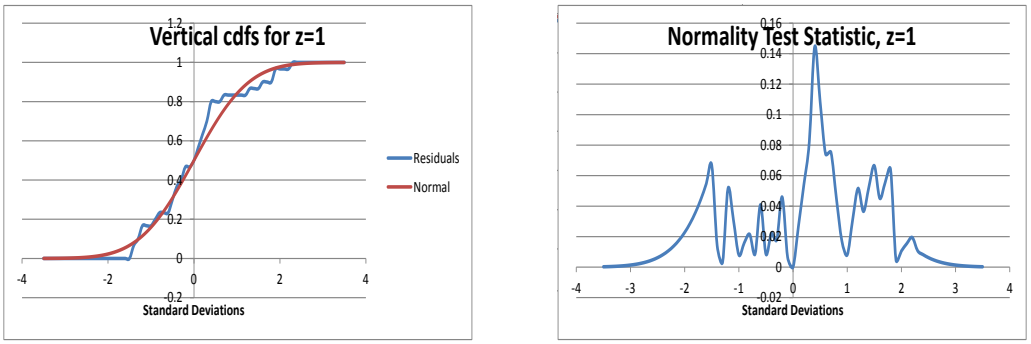

The pseudo-random samples were used to generate a p.d.f. and a c.d.f. for w and these were used to calculate statistics for w at levels $z = 1$, 2, and 3 for selected values of the distance from the vortex center r. Shannon's information content of the p.d.f. for w was also calculated. The statistics for w at $z = 1$,2, and 3 are given in Table 8.23 and Table 8.24 for selected values of r. In the tables, $w(r)$ is the estimated value of w using the Wood-White vortex 2 model. Table 8.23 contains data using parameter pairs from the grid

with spacing 0.01. Table 8.24 contains data using parameters pairs from the pseudo-random sample.

Table 8.23: Statistics for w, Grid Sample

height z	radius r	$w(r)$	μ_w	σ_w	$I(w)$
1	0.538	0.8330	0.9001	0.1687	0.1708
1	0.846	0.4252	0.4332	0.0478	0.2451
1	1.231	0.1124	0.0817	0.1023	0.2436
1	1.538	0.0159	0.0084	0.0922	0.1633

Table 8.24: Statistics for w, Pseudo-Random Sample

height z	radius r	$w(r)$	μ_w	σ_w	$I(w)$
1	0.538	0.8330	0.9003	0.1696	0.1691
1	0.846	0.4252	0.4330	0.0479	0.2453
1	1.231	0.1124	0.0824	0.1022	0.2423
1	1.538	0.0159	0.0090	0.0923	0.1014

The means and standard deviations for w were used to create 80% error bars. Example plots are given in figure 8.19. The first plot shows a comparison between the c.d.f.s for w with the uniform distribution and the distribution from the Davies-Jones data at a distance of $r = 0.538$ from the vortex center. This plot demonstrates the value of the data in determining the value of w. The second plot shows error bars around w using the two distributions over all the values of r where $0 \leq r \leq 2.231$.

The large error bars are a result of the large uncertainty in tangential wind v and radial wind u. This uncertainty can be reduced further with uncorrelated and Gibbs sampling. The data in table 8.25 is from level $z = 1$. Table 8.25 gives the actual value of w, the estimation of w from the sample and the standard deviation of w and shows the reduction of the standard deviation of w given a sample with more information. Table 8.25 also reveals the close agreement between data obtained from sample S_2 and data obtained from much

Figure 8.19: Vertical cdf and Error Bars

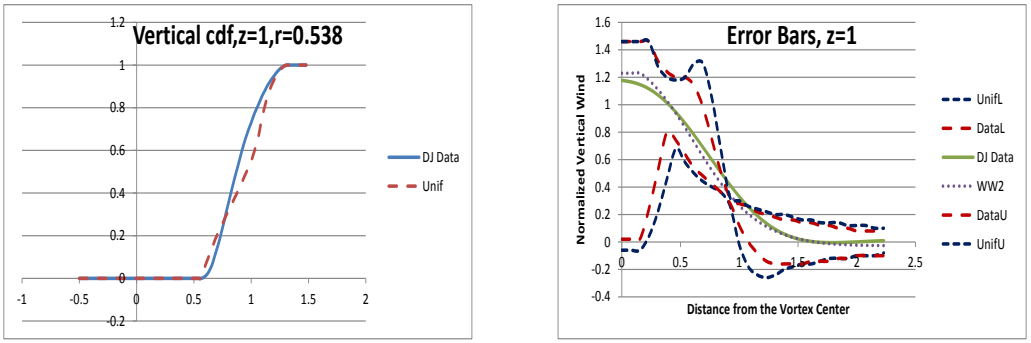

larger samples discussed earlier. This verifies the ability to predict the vertical wind w from small samples that could possibly be obtained in a real-time system.

Table 8.25: Statistics for w from Small Samples

Sample	radius r	$w(r)$	μ_w	σ_w	$I(w)$
S_2	0.538	0.833	0.904	0.169	0.150
S_2	0.846	0.425	0.434	0.047	0.231
S_2	1.231	0.112	0.077	0.101	0.226
S_2	1.538	0.016	0.002	0.092	0.141
S_3	0.538	0.833	0.874	0.150	0.329
S_3	0.846	0.425	0.425	0.038	0.360
S_3	1.231	0.112	0.098	0.087	0.380
S_3	1.538	0.016	0.020	0.084	0.299
S_4	0.538	0.833	0.873	0.143	0.400
S_4	0.846	0.425	0.423	0.031	0.486
S_4	1.231	0.112	0.096	0.077	0.484
S_4	1.538	0.016	0.012	0.079	0.326

The Gibbs data set S_3 contains more information than the pseudo-random sample. Figure 8.20 shows the c.d.f.s generated from samples S_1 and S_3 at level $z = 1$ and the previous graph generated from the pseudo-random sample. This comparison illustrates the results of using a data set with more information.

The following results are based on the Wood-White 2 vortex model, the benchmark Davies-Jones data set and the non-cylindrical case. The maximum

Figure 8.20: Pseudo-random sample and Gibbs c.d.f.s

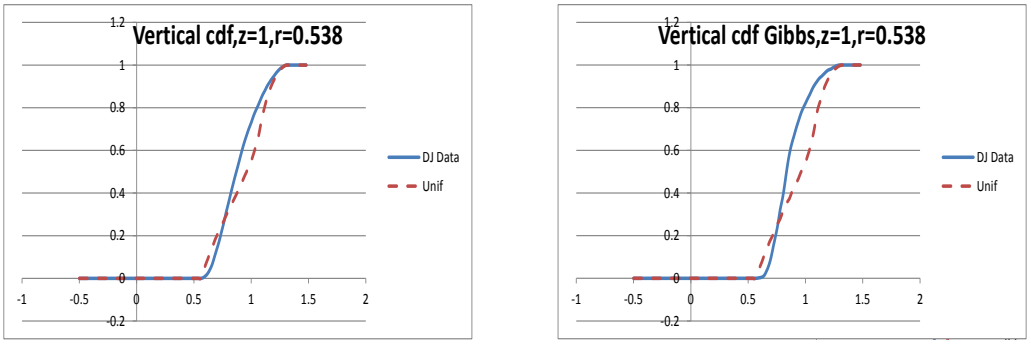

tangential wind vertical profile was assumed.

1. The residuals can be assumed to be normally distributed with zero mean and equal variances. They are correlated, therefore any statistical tests must adjust the degree of freedom.

2. It was shown that good estimates of the parameters in the Wood-White 2 vortex model provided good estimates of the tangential,radial and vertical profiles using a subset of the Navier-Stokes system of equations.

3. Uncertainty in the parameter estimates results in uncertainty in the profile estimates.

4. The marginal distributions for a and b were skewed, so the means are biased. It is important to notice that the standard deviations are large, so that the estimates are uncertain.

5. The importance of parameter b is evident throughout the profile. The importance of parameter a grows and becomes more important than b at the end of the profile.

6. Both parameters are essential in estimation of the tangential wind profile because they contain critical information about the profile.

7. The greater the information from the benchmark Davies-Jones data set in the sample, the greater the information in u, v and w.

8. The Wood-White 2 vortex model is more sensitive to parameter b which controls the inner profile than to parameter a which controls the end of the profile.

9. Sensitivity with respect to ν is largest near the location of maximum tangential wind.

Chapter 9

Conclusions

The analysis methods discussed in this paper were applied to the Wood-White 2 tangential vortex model and are intended for use on other tangential vortex models. The Davies-Jones data set was used as a benchmark data set for the uncertainty analysis because it is considered a validated and verified data set. The Wood-White 2 vortex model was selected for analysis because of its ability to capture the information in the Davies-Jones data set and its small number of parameters so that a thorough analysis could be done. This allowed for exploration of the utility of small sample sizes to provide information to a real-time system. Future work would necessarily involve analysis of other models and incorporation of other benchmark data sets.

The Wood-White 2 tangential vortex model contains two parameters a and b. Non-linear least squares were used to estimate the parameters of the Wood-White 2 tangential vortex model using the Davies-Jones data set. The Wood-White vortex 2 tangential wind model approximates the benchmark Davies-Jones data closely with the amount of data provided by the data set. The residuals of the errors are most likely correlated and this will probably be the case for all models. An assumption can be made that the residuals are normally distributed, therefore non-linear least squares analysis is appropriate. It was determined that parameter b which controls the shape of the inner core of an atmospheric vortex contains more information about the tangential wind profile

than parameter a which controls the decay of the vortex beyond the point of maximum tangential wind, however, the end of the profile is more sensitive to parameter a. In conclusion, both parameters are essential in estimation of the tangential wind profile because they contain critical information about the profile. The marginal distributions of the parameters revealed large variances for the parameters. The variances were reduced by using samples containing more information from the data set in the analysis. Reduction in the variance of the parameters could be accomplished after analysis with more benchmark data sets. Discriminant analysis could categorize data to reduce the size of the admissible parameter space. For example, data categories could consist of hurricanes, and one- and two- cell tornadoes. Also, the techniques in this paper could be used to eliminate unnecessary parameters in other tangential wind models.

Radial and vertical winds were estimated using the Wood-White 2 vortex model to estimate tangential wind with the Navier-Stokes tangential momentum equation and conservation of mass. These approximations were compared to the Davies-Jones data set. Under the z-dependent case with the appropriate z-dependent profile, the approximations compared favorably to the Davies-Jones data set. The uncertainty in prediction of the tangential profile v was evaluated in terms of the propagation of uncertainty in the model parameters a and b. The uncertainty in v was then propagated into the uncertainty of u which also incorporated a new parameter ν with its own statistical properties. Finally, the uncertainty analysis of vertical w was performed which was dependent on a, b, v, ν and u. Large uncertainties in the parameters lead to large uncertainties in the prediction of tangential v, radial u and vertical w. Samples containing information content, such as the uncorrelated sample

taken from the marginal distributions and the Gibbs sample which includes the correlation, reduced uncertainties in the estimates of u, v and w. It was shown that small samples can be used in a real-time system.

A summary of information content is given in table 9.1. Observe that all the selected distances from the vortex center have high information content for u, v and w. In conclusion, data received from these regions would be valuable in determining wind profiles. Data received from the distance of maximum tangential velocity has high information content for u and w. This does not show up for v because of the forced normalization of the tangential wind profile model. This does not mean that data in this location is not important for v. The information content for v would show up in the estimation of the actual value of the maximum velocity and in the location of the maximum tangential wind. It can be seen that data approximately halfway between the vortex center and the radius of maximum tangential wind provides the most information to radial, tangential and vertical wind profiles. In general, information content is high throughout the profiles and the correlation at radial distances in close proximity is evident. The large information content of v comes from the data through the parameters and from the form of the model used to approximate the tangential wind profile. The Gibbs sample contains more information from the benchmark data set than the uniform sample by including the correlation between the parameters and sampling from the actual joint distribution of the parameters. This resulted in reduced variances and greater information content in radial, tangential and vertical wind estimates.

Questions remain about other methods that can be used to reduce the variance in model parameters which will lead to reduced variance in model pre-

Table 9.1: Information with Two Different Samples

	Uniform			Gibbs		
radius r	$I(u)$	$I(v)$	$I(w)$	$I(u)$	$I(v)$	$I(w)$
0.077	0.134	0.118	0.159	0.349	0.371	0.448
0.231	0.175	0.173	0.178	0.432	0.441	0.449
0.385	0.215	0.202	0.219	0.486	0.510	0.459
0.538	0.231	0.225	0.150	0.512	0.538	0.400
0.692	0.152	0.242	0.240	0.285	0.548	0.545
0.846	0.209	0.230	0.231	0.411	0.504	0.486
1.000	0.206	0.000	0.243	0.404	0.000	0.499
1.154	0.236	0.223	0.234	0.470	0.450	0.495
1.308	0.236	0.240	0.212	0.485	0.506	0.452
1.462	0.229	0.234	0.168	0.484	0.510	0.389
1.615	0.222	0.226	0.119	0.492	0.511	0.294
1.769	0.214	0.218	0.109	0.479	0.500	0.204
2.000	0.202	0.208	0.086	0.442	0.484	0.157

dictions. Also, the amount and location of data that can provide accurate predictions of tangential, radial and vertical winds are of value to pursue. Information theory is often used for model selection. Models could be selected based on their ability to capture the information in the available data. Different models could be selected at difference locations in the vortex to provide maximum information to the scientist about tangential, radial and vertical components of the vortex wind field.

Bibliography

[1] Akaike, H., 1981: Likelihood of a model and information criteria. *Journal of Econometrics*, **16**, 3-14.

[2] Bates, D. M. and Watts, D. G., 2007: *Nonlinear Regression Analysis and Its Applications*, John Wiley and Sons, New York.

[3] Beck, J. V. and Arnold, K. J., 1977: *Parameter Estimation in Engineering and Science*, John Wiley and Sons, New York.

[4] Burgers, J. M., 1948: A mathematical model illustrating the theory of turbulence. *Adv. Appl. Mech.*, **1**, 197-199.

[5] Burnham, K. P. and Anderson, D. R., 2002: *Model Selection and Multimodel Inference: A Practical Information-Theoretic Approach*, (2nd edition), Springer-Verlag, New York.

[6] Butcher, J. C., 2008: *Numerical Methods for Ordinary Differential Equations*,(2nd edition), John Wiley and Sons, Ltd, The Atrium, Southern Gate, Chichester West Sussex, England.

[7] Carrier, G. P. and Pearson, C. E., 1976: *Partial Differential Equations Theory and Technique*, Academic Press, New York.

[8] Claeskens, G., Hjort, N. L., 2009: *Model Selection and Model Averaging*, Cambridge University Press, New York.

[9] Corder, G. W., Foreman, D. I., 2009: *Nonparametric Statistics for Non-Statistians*, John Wiley and Sons, Inc., Hoboken, New Jersey.

[10] Cover, T. M. and Thomas, J. A., 2006: *Elements of Information Theory*, John Wiley and Sons, Inc., New Jersey.

[11] Davies-Jones, R. P., 2007: Can a Descending Rain Curtain in a Supercell Instigate Tornadogenesis Barotropically?. *J. Atmos. Sci.*, **65**, 2469-2497.

[12] Gibbons, J. D., 1985: *Nonparametric Statistical Inference*,(2nd edition), Marcel Dekker, Inc., New York.

[13] Hills, R. G., Trucano, T. G., 1999: Statistical Validation of Engineering and Scientific Models: Background. Technical Report SAND99-1256, Sandia National Laboratories.

[14] Jarque, C. M. and Bera, A. K. 1987: A test for normality of observations and regression residuals. *International Statistical Review*, **55(2)**, 163-172.

[15] Kundu, P. K. and Cohen, I. M., 2004: *Fluid Mechanics*,(3rd edition), Elsevier Academic Press, New York.

[16] Lilliefors, H. W., 1967: On the Kolmogorov-Smirnov test for normality with mean and variance unknown. *J. Amer. Statist. Assoc.*, **62**, 399-402.

[17] McKay, M. D., 1995: Evaluating Prediction Uncertainty. Technical Report NUREG/CR-6311, US Nuclear Regulatory Commission and Los Alamos National Laboratory.

[18] Morrison, D. F., 1976: *Multivariate Statistical Methods*, McGraw-Hill Book Company, New York.

[19] Rankine, W. J. M., 1882: *A Manual of Applied Physics*, (10th edition), Charles Griff and Company, London.

[20] Rott, N., 1958: On the viscous core of a line vortex. *Z. Angew Math. Physik*, **9**, 543-553.

[21] Roussas, G. G., 1973: *A First Course in Mathematical Statistics*, Addison Wesley Publishing Company, Reading, Massachusetts.

[22] Saltelli, A., Chan, K., and Scott, E. M., 2000: *Sensitivity Analysis*, John Wiley and Sons, LTD, Chichester.

[23] Schweppe, F. C., 1973: *Uncertain Dynamic Systems*, Prentice-Hall, Inc., Englewood Cliffs, New Jersey.

[24] Shannon, C. E., 1948: A mathematical theory of communication. *Bell System Tech. J.*, **27**, 379-423.

[25] Sugiura, N., 1978: Further analysis of the data by Akaike's information criterion and the finite corrections. *Communications in Statistics, Theory and Methods*, **A7**, 13-26.

[26] Sullivan, R. D., 1959: A two-cell vortex solution of the Navier-Stokes equations. *J. Aerospace Sci.*, **26**, 767-768.

[27] Tarantola, A. and Valette, B, 1982: Inverse Problems = Quest for Information. *J. Geophys.*, **50**, 159-170.

[28] Trapp, R. Jeffrey, 1999: A clarification of vortex breakdown and tornadogenesis. *Monthly Weather Review*, **128**, 888-895.

[29] Trapp, R. Jeffrey and Davies-Jones, R. P., 1997: Tornadogenesis with and without a dynamic pipe effect. *J. Atmos. Sci.*, **54**, 113-133.

[30] Trucano, T. G., Swiler, L. P. Igusa, T. Oberkampf, W. I. and Pilch, M., 2006: Calibration, validation, and sensitivity analysis: What's what. *Reliability Engineering and System Safety*, **91**, 1331-1357.

[31] Vanyo, J. P., 1993: *Rotating Fluids in Engineering and Science*, Dover Publications, Inc., Mineola, New York.

[32] Wood, Vincent T. and White, Luther W., 2011: A new parametric model of vortex tangential-wind profiles: development, testing and verification. *J. Atmos. Sci.*, **68**, 990-1006.

Appendices

Appendix A

Derivatives of the Vertical Wind Profile

The vertical wind profile ψ and the derivatives of ψ are

$$
\begin{aligned}
\psi(z) = {} & \tanh\left(\frac{A_1 z}{H}\right) \tanh\left(A_2\left(1-\frac{z}{H}\right)\right) \\
\psi_z = {} & \frac{A_1}{H}\operatorname{sech}^2\left(\frac{A_1 z}{H}\right) \tanh\left(A_2\left(1-\frac{z}{H}\right)\right) \\
& -\frac{A_2}{H}\tanh\left(\frac{A_1 z}{H}\right) \operatorname{sech}^2\left(A_2\left(1-\frac{z}{H}\right)\right) \\
\psi_{zz} = {} & -2\left(\frac{A_1}{H}\right)^2 \operatorname{sech}^2\left(\frac{A_1 z}{H}\right) \tanh\left(\frac{A_1 z}{H}\right) \tanh\left(A_2\left(1-\frac{z}{H}\right)\right) \\
& -2\left(\frac{A_1}{H}\right)\left(\frac{A_2}{H}\right) \operatorname{sech}^2\left(\frac{A_1 z}{H}\right) \operatorname{sech}^2\left(A_2\left(1-\frac{z}{H}\right)\right) \\
& -2\left(\frac{A_2}{H}\right)^2 \tanh\left(\frac{A_1 z}{H}\right) \operatorname{sech}^2\left(A_2\left(1-\frac{z}{H}\right)\right) \tanh\left(A_2\left(1-\frac{z}{H}\right)\right) \\
\psi_{zzz} = {} & -2\left(\frac{A_1}{H}\right)^3 \operatorname{sech}^4\left(\frac{A_1 z}{H}\right) \tanh\left(A_2\left(1-\frac{z}{H}\right)\right) \\
& +4\left(\frac{A_1}{H}\right)^3 \operatorname{sech}^2\left(\frac{A_1 z}{H}\right) \tanh^2\left(\frac{A_1 z}{H}\right) \tanh\left(A_2\left(1-\frac{z}{H}\right)\right) \\
& +6\left(\frac{A_1}{H}\right)^2\left(\frac{A_2}{H}\right) \operatorname{sech}^2\left(\frac{A_1 z}{H}\right) \tanh\left(\frac{A_1 z}{H}\right) \operatorname{sech}^2\left(A_2\left(1-\frac{z}{H}\right)\right) \\
& -6\left(\frac{A_1}{H}\right)\left(\frac{A_2}{H}\right)^2 \operatorname{sech}^2\left(\frac{A_1 z}{H}\right) \operatorname{sech}^2\left(A_2\left(1-\frac{z}{H}\right)\right) \tanh\left(A_2\left(1-\frac{z}{H}\right)\right) \\
& -4\left(\frac{A_2}{H}\right)^3 \tanh\left(\frac{A_1 z}{H}\right) \operatorname{sech}^2\left(A_2\left(1-\frac{z}{H}\right)\right) \tanh^2\left(A_2\left(1-\frac{z}{H}\right)\right) \\
& +2\left(\frac{A_2}{H}\right)^3 \tanh\left(\frac{A_1 z}{H}\right) \operatorname{sech}^4\left(A_2\left(1-\frac{z}{H}\right)\right)
\end{aligned}
$$